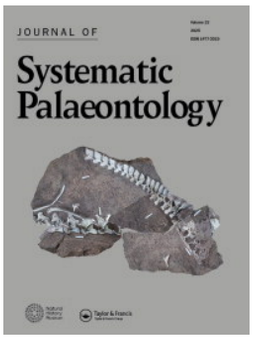

Journal of Systematic Palaeontology

ISSN: 1477-2019 (Print) 1478-0941 (Online) Journal homepage: www.tandfonline.com/journals/tjsp20

The first record of *Pliotragus* (Artiodactyla: Bovidae) in the Early Pleistocene of eastern Asia; contribution to its systematics, palaeohabitat and palaeobiogeography

Weipeng Bai, Roman Croitor, Limin Zhang & Wei Dong

To cite this article: Weipeng Bai, Roman Croitor, Limin Zhang & Wei Dong (2025) The first record of *Pliotragus* (Artiodactyla: Bovidae) in the Early Pleistocene of eastern Asia; contribution to its systematics, palaeohabitat and palaeobiogeography, Journal of Systematic Palaeontology, 23:1, 2518101, DOI: 10.1080/14772019.2025.2518101

To link to this article: https://doi.org/10.1080/14772019.2025.2518101

Journal of Systematic Palaeontology, 2025
Vol. 23, No. 1, 2518101
http://dx.doi.org/10.1080/14772019.2025.2518101

The first record of *Pliotragus* (Artiodactyla: Bovidae) in the Early Pleistocene of eastern Asia; contribution to its systematics, palaeohabitat and palaeobiogeography

Weipeng Bai[a,b], Roman Croitor[c], Limin Zhang[d] and Wei Dong[d]*

[a]*College of History and Culture, Hebei Normal University, Shijiazhuang 050024, PR China;* [b]*Hebei Key Laboratory of East Asian Human Origin and Civilization Research, Hebei Normal University, Shijiazhuang 050024, PR China;* [c]*Laboratory of Terrestrial Vertebrates, Institute of Zoology, State University of Moldova, Chişinău MD-2028, Republic of Moldova;* [d]*Key Laboratory of Vertebrate Evolution and Human Origins of Chinese Academy of Sciences, IVPP, CAS, Beijing 100044, PR China*

(Received 3 September 2024; accepted 19 May 2025)

Pliotragus is a large-sized caprin within Bovidae, primarily known from the Late Pliocene to the Middle Pleistocene of Europe. To date, only a single site with this genus has been discovered in western Asia (Sarikol Tepe, Ankara, Turkey). It remains poorly understood due to insufficient material and study. In this paper, we report the first record of *Pliotragus* in eastern Asia (Xinyaozi locality, China) and compare it with some related taxa. The new specimens are similar to *P. ardeus* in cranial morphology and tooth measurements. However, considering certain differences between the horncore from Xinyaozi and that of its European counterparts, we classified the new material as *Pliotragus* cf. *ardeus*. Based on previously discovered material and our new specimens, we performed a Bayesian total-evidence dating analysis to determine the taxonomic status of the species. The results show that it should be placed in Caprini, clustering with the clade of *Capricornis-Ovibos-Euceratherium*, indicating closer relationships with *Ovibos* rather than *Rupicapra*, as previously proposed. We discuss whether *P. ardeus* might be a synonym of *Sinoryx bombifrons* based on similarities in their morphology and size. Additionally, we reconstructed its diet and habitat using dental and limb bone morphometric features. *Pliotragus ardeus* was likely a browse-dominated or mixed feeder that might have been adapted to both mountainous and plain regions, with intermediate diet and habitat preferences. Finally, we summarized its biostratigraphic position and palaeobiogeography, inferring that it dispersed from eastern Asia to Europe during the late Late Pliocene to early Early Pleistocene, probably triggered by increased glaciation.

Keywords: *Pliotragus*; eastern Asia; Early Pleistocene; taxonomy; palaeohabitat; palaeobiogeography

Introduction

Pliotragus ardeus is a prominent enigmatic caprine species, distinguished by a suite of distinctive ecomorphological traits lacking ecological parallels within contemporary faunal assemblages (Duvernois & Guérin, 1989). With a body mass reaching approximately 200 kg (Croitor et al., 2024), *Pliotragus ardeus* holds the distinction of being one of the largest species within Caprini. Its horncores are characterized by their short, stout nature, exhibiting a subtle curvature. Initially discovered from the Late Pliocene of Perrier, France, the species was originally reported as *Antilope ardea*, based on the discovery of a maxilla, a fragmentary skull with partially preserved horncores, and a metacarpal bone (Depéret, 1884). The initial classification of this species within the genus *Antilope* might stem from the presence of an unusually elongated and slender metacarpal bone, which was deemed most likely to belong to a cervid based on its measurements (Duvernois & Guérin, 1989). Schaub (1923) subsequently introduced a new genus name, *Deperetia*, for this species, although without providing an explicit diagnosis, and noted the ambiguous systematic position of the genus. Later, Kretzoi (1941) proposed the replacement of the generic name *Deperetia* with *Pliotragus* because the former was already preoccupied by a pectenid.

To date, *Pliotragus* encompasses two recognized species: *P. ardeus* (Depéret, 1884) and *P. macedonicus* Crégut-Bonnoure and Tsoukala, 2005. The latter species was identified from the Middle Pleistocene of Greece, documented solely from a few isolated upper teeth, with no subsequent discoveries reported. Beyond the European fossil record of *Pliotragus*, Kostopoulos and

*Corresponding author. Email: dongwei@ivpp.ac.cn

Published online 23 Jul 2025

Sen (1999) documented some isolated upper and lower teeth from Turkey, tentatively assigned to cf. *Pliotragus* based on their morphological resemblance and dimensional congruence with the type species. This represented the initial documentation of the genus within western Asia. Recently, Crégut-Bonnoure (2025) reviewed old collections and described some new specimens of this species discovered in Europe, giving us some important morphological and biometric information. However, *Pliotragus* still remains a poorly understood bovid genus, due to a lack of consensus regarding its systematic classification, uncertain origins, and incomplete data on its geographical distribution.

In this study, we present the first fossil record of *Pliotragus* in eastern Asia. We undertake a detailed comparative analysis of *Pliotragus* with some related taxa, elucidating its taxonomic status, palaeoenvironmental preferences, and palaeobiogeographical significance. Our study represents a significant expansion of our understanding of this remarkable enigmatic bovid species, meaningfully augmenting our knowledge of the morphology, individual variation, diagnostic characteristics of *Pliotragus*, and extending its geographical range to encompass eastern Asia.

Geological setting

The fossil locality is located along the Xinyaozi Ravine within the Xionger Mountains in Shanxi Province, China. The mountains demarcate the north-western boundary of the Nihewan Basin (Fig. 1). The discovered specimens predominantly originated from a stratigraphical unit

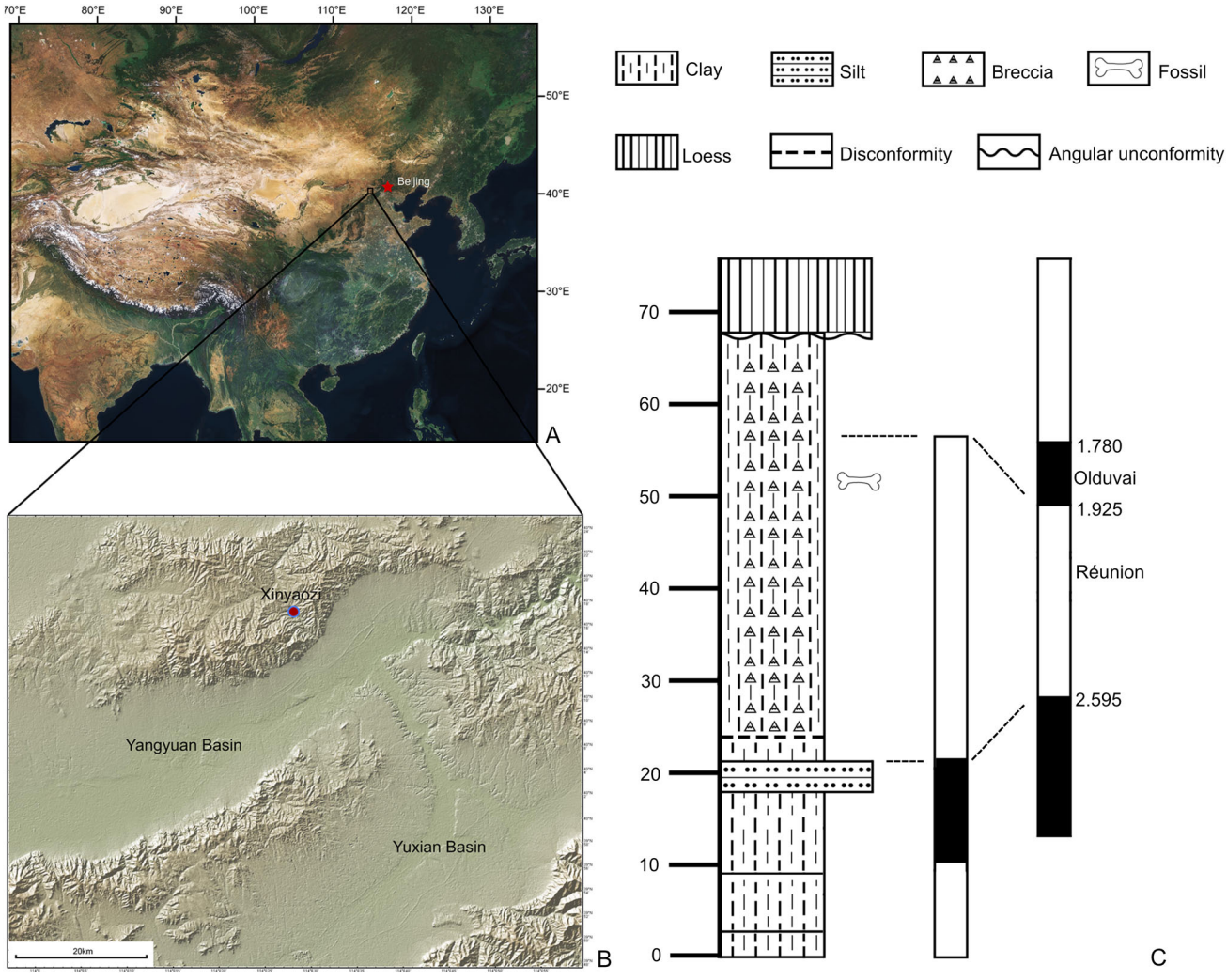

Figure 1. **A, B,** geographical location of Nihewan Basin (the red dot indicates the studied fossil locality). **C,** stratigraphical section of Xinyaozi with magnetostratigraphical ages (in Ma).

comprising brown clay, intermixed with breccia and multiple strata of flowstones, spanning a thickness of 30–40 m (Liu, 1989). The horizon yielding the fossils was palaeomagnetically dated to approximately 2.6–1.95 million years ago (Liu, 1989). Preliminary identifications of the species belonging to the Xinyaozi fauna confirms its age as early to middle Early Pleistocene (Qiu, 2002; Qiu et al., 2002). Notably, systematic studies on the Xinyaozi fauna have focused on taxa such as Hyracoidea (Qiu et al., 2002), Perissodactyla (Deng & Xue, 1999; Dong et al., 2021; Dong et al., 2023; Qiu, 2002), Eulipotyphla (Bai et al., 2022), partially Bovidae (Bai et al., 2019; Bai, Dong, et al., 2024; Bai, Wang, et al., 2024), and Cervidae (Dong et al., 2019; Dong et al., 2020), while other material is still under study.

Material and methods

The material described in this paper is housed in the Collection House of the Institute of Vertebrate Paleontology and Paleoanthropology, Chinese Academy of Sciences, Beijing (IVPP). The terminology used for teeth follows Bärmann and Rössner (2011). The classification of Bovidae follows that of Groves and Grubb (2011). Measurements of horncores and skulls adhere to the methodologies outlined by Teilhard de Chardin and Trassaert (1938), Bolomey (1965), Duvernois and Guérin (1989) and Crégut-Bonnoure (2025). The plots and Simpson's logarithm ratio diagram were generated using ChiPlot (https://www.chiplot.online/index.html). The Cluster Analysis and Discriminant Function Analysis (DFA) based on the mesowear scores were performed using PAST v. 5.0 (Hammer et al., 2001) and SPSS v. 26.0. The principal component analysis (PCA) of bibliographical data on limb bones of selected bovids was firstly conducted by using SPSS to standardize the dataset, then using OriginPro v. 2024 to analyse the standardized dataset. Measurements were taken using a digital calliper with a precision of 0.01 mm.

Phylogenetic analysis was performed to assess the systematic placement of *Pliotragus* cf. *ardeus* from Xinyaozi and *Pliotragus ardeus* from Europe within the Bovidae. Bayesian total-evidence dating was performed with combined morphological (established by Bärmann [2012] with the character states of some species revised based on Wang et al. [2023]) and molecular (Hassanin et al., 2012) data using MrBayes v. 3.2.7 (Ronquist, Teslenko, et al., 2012). Bayesian analysis with tip-dating under relaxed clock model and fossilized birth-death model was adopted (Ronquist, Klopfstein, et al., 2012; Zhang et al., 2016). The morphological blocks were analysed using the mkv model (Lewis, 2001) and the molecular blocks were analysed using the GTR+gamma model. The analysis was run for a total of 100,000,000 generations. The morphological character states of *Pliotragus* cf. *ardeus* and *Pliotragus ardeus* were coded according to the Xinyaozi specimens and the remains described and illustrated by Bolomey (1965), Croitor et al. (2024), Depéret (1884), Duvernois and Guérin (1989), Schaub (1923) and Crégut-Bonnoure (2025) (see Bai et al., 2025 for phylogenetic data).

Tooth measurements and the hypsodonty index were obtained to investigate the diet of *Pliotragus* cf. *ardeus* from Xinyaozi and *P. ardeus* from Europe. This analysis used the datasets from Mendoza et al. (2002) (see Supplemental material Table S5). Feeding types of extant Bovidae were classified following Mendoza et al. (2002). To further estimate the dietary preferences of *P. ardeus*, we performed a mesowear analysis based on the m2. The mesowear scoring system refers to Fraser et al. (2014). The dataset follows Carranza-Castañeda and Jiménez-Hidalgo (2021) and was converted to percentages (see Supplemental material Table S6). The dataset was analysed using hierarchical clustering with Euclidean distance and complete linkage method, and discriminant function analysis. Additionally, we selected metacarpal and radius measurements of *P. ardeus* found in Europe (no postcranial bones from Xinyaozi have been ascribed to the studied taxon) for a principal component analysis to estimate their ecomorphological adaptations (Croitor et al., 2024; Duvernois & Guérin, 1989; Guérin, 1965; Kostopoulos, 1997; Sher, 1997; Tong et al., 2022) (see Supplemental material Tables S7, S8).

Systematic palaeontology

Order **Artiodactyla** Owen, 1848
Family **Bovidae** Gray, 1821
Subfamily **Antilopinae** Gray, 1821
Tribe **Caprini** Simpson, 1945
Genus ***Pliotragus*** Kretzoi, 1941
Pliotragus* cf. *ardeus (Depéret, 1884)
(Figs 2–4; Tables 1–3)

1884 *Antilope ardea* Depéret: 252, pl. 8, fig. 3.
1923 *Deperetia ardea* Schaub: 287–291, figs 3, 4.
1941 *Pliotragus* nov. gen. Kretzoi: 349.
1961 *Pliotragus* Viret: 1074.
1965 *Deperetia ardea* Guérin.
1965 *Pliotragus ardeus* Bolomey: 315–323, pl. 1–4.
1971 *Pliotragus* (= *Deperetia*) *ardeus* Gentry: 281–282.
1989 *Pliotragus ardeus* Duvernois et Guérin: 350–355.
2024 *Pliotragus ardeus* Croitor et al.: 488–492, fig. 2.

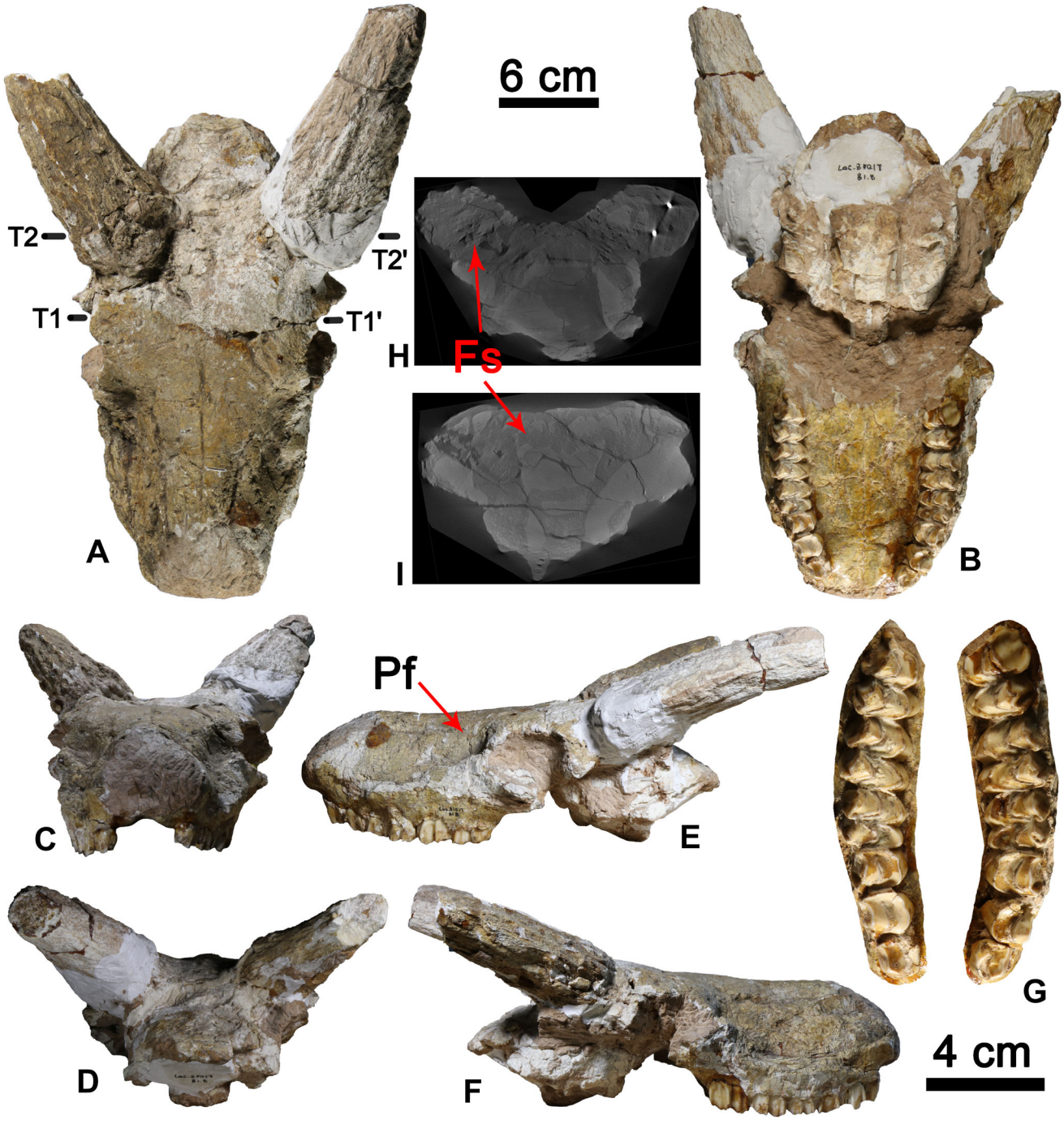

Figure 2. A well-preserved skull of *Pliotragus* cf. *ardeus* (V 31263.1) from Xinyaozi. **A,** dorsal view; **B,** ventral view; **C,** anterior view; **D,** posterior view; **E,** left lateral view; **F,** right lateral view; **G,** occlusal view of upper teeth; **H,** CT image of cross-section through T1–T1'; **I,** CT image of cross-section through T2–T2'. **Abbreviations: Fs**, frontal sinus; **Pf**, preorbital fossa. 6 cm scale bar for A–F; 4 cm scale bar for G. CT images not shown to scale.

Holotype. A broken left maxilla with P2–M3 (Depéret, 1884, plate 8, Fig. 3). The holotype has been lost, but a cast is housed at Basel Museum in Switzerland (Duvernois & Guérin, 1989).

Type locality. Perrier-Etouaires in France. Late Pliocene to Early Pleistocene.

Diagnosis (modified from Duvernois & Guérin, 1989). Large caprine. Horncores are short, robust, divergent

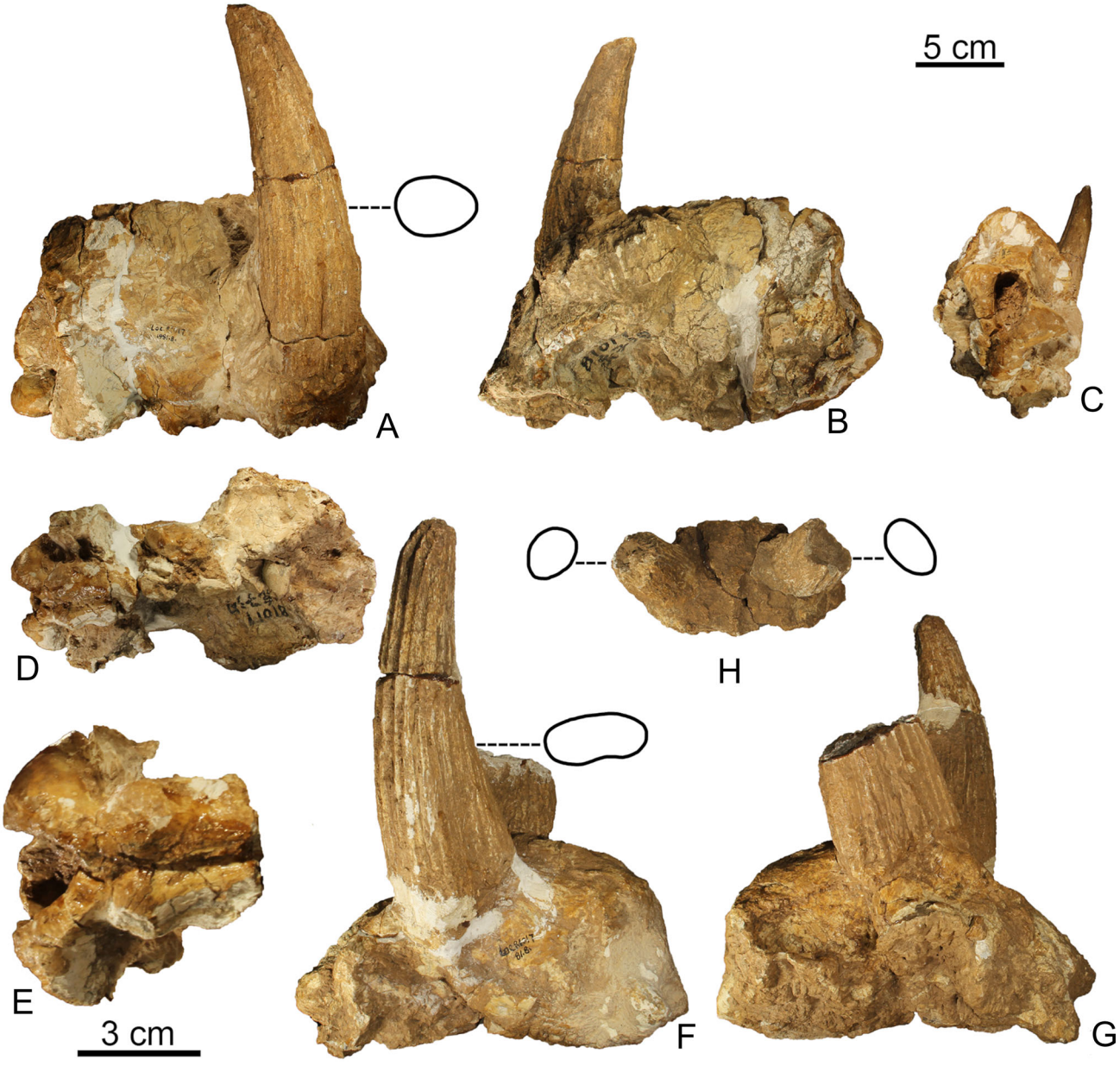

Figure 3. Broken skulls of *Pliotragus* cf. *ardeus* (V 31264.1–3) from Xinyaozi. **A–E,** V 31264.1. **F, G,** V 31264.2. **H,** V 31264.3. **A,** right lateral view (cross-section of horncore); **B,** left lateral view; **C,** posterior view; **D,** ventral view; **E,** magnified basioccipital part. **F,** left lateral view (cross-section of horncore); **G,** right lateral view. **H,** dorsal view (cross-section of horncore). 5 cm scale bar for A–D and F–H; 3 cm scale bar for E.

from base to tip, located immediately behind the orbits, grooved longitudinally, oriented outwards and upwards and slightly inwards at their distal portion. The anterior rim of basal horncores is located laterally, whereas the posterior rim of basal horncores is positioned medially. Occipital surface wide. Rectangular basioccipital with two pairs of relatively developed tuberosities. Upper molars have enamel island in the middle of the tooth, but lack entostyle column. The p4 is highly molarized, with the fusion of anterior conid and mesolingual conid in the first lobe, and posterolingual conid and posterior stylid in the second lobe. The anterior cingulid is weak or absent in the lower molars, with small parastylid and metastylid and weak lingual conid folds. The ectostylid is developed or absent in m1.

Referred material. A broken skull with a pair of horncores (V 31263.1); two laterally compressed skulls without facial parts (V 31264.1, 2); a fragmental frontal with a pair of basal horncores (V 31264.3); an

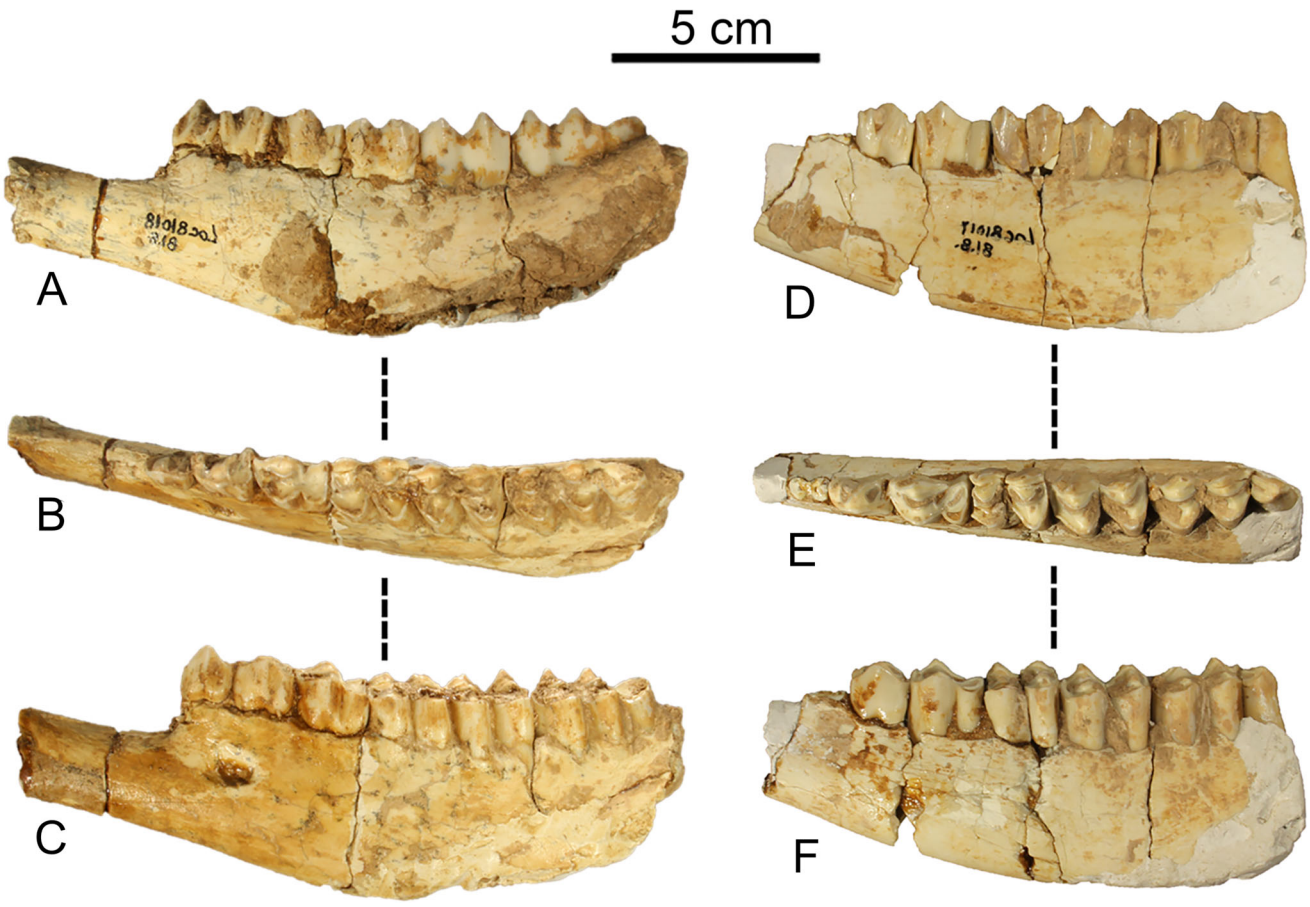

Figure 4. Two broken left mandibles of *Pliotragus* cf. *ardeus* from Xinyaozi. **A–C,** V 31263.2; **D–F,** V 31263.3. Images from top to bottom show medial, occlusal and lateral views.

incomplete left hemimandible with p2–m3 (V 31263.2); an incomplete left hemimandible with p3–m3 (V 31263.3). Except for V 31263.2 unearthed from Locality 81018, all the other samples were discovered at Locality 81017 along the Xinyaozi Ravine.

Occurrence. Localities 81017 and 81018 along the Xinyaozi Ravine, Tianzhen County, China. Early Pleistocene.

Description

Skull. V 31263.1 is an incomplete skull with a pair of horncores, discovered from Locality 81017. The snout, occiput and basicranium are not preserved (Fig. 2A). The skull is frontoventrally distorted, with the surface of the horncores severely eroded. Preservation is better on the left horncore compared to the right one. The horncore is straight from the base to the middle portion, with a slight medial bend at the upper end and rapid tapering towards the tip. Its cross-section is oval shaped with mediolateral compression. The anteroposterior axis of the cross-section is at an angle of 35° to the sagittal plane, with the anterior part of the basal horncores located laterally, whereas the posterior part of the basal horncores is situated medially. There are some well-developed longitudinal grooves on the anterior and lateral surfaces of the horncores. The horncores are well-separated at the base, forming a 55° angle of divergence. The horncore is situated at the posterior rim of the orbit and is permeated with the developed frontal sinus at its base (Fig. 2H, I). The snout is filled with matrix. The surface of the skull is weathered, with sutures vaguely visible. In dorsal view (Fig. 2A), the facial part appears slightly wide. The fronto-nasal suture is positioned at the same level as the posterior rim of the preorbital fossa. The supraorbital foramen is small and shallow, elliptical in shape. The orbital rim is partially broken, but likely weakly protruding outward. The frontal bone anterior to the horncores is flat without any bulging. In lateral view (Fig. 2E, F), the preorbital fossa is relatively large, positioned atop the M2 and M3. The anterior rim of the orbit is on top of the distal lobe of M3. The braincase is short, bending ventrally from the interhorncore and inclining with the facial part at an angle of approximately 150°. In ventral/palatal view (Fig. 2B), the

Table 1. Measurements (in mm) of the skull of *Pliotragus* cf. *ardeus* from Xinyaozi and other related taxa.

	Pliotragus cf. *ardeus*				*Ovis* sp.	*Pliotragus ardeus*	*P. ardeus*	*P. ardeus*	*Pliotragus ardeus*	*Sinoryx bombifrons*
	V 31263.1	V 31264.1	V 31264.2	V 31264.3	Udunga[(1)]	Senèze[(2)]	Irimești[(3)]	Senèze[(4)]	Senèze and Dacian Basin[(5)]	Yushe[(6)]
1	133.32			130.72				107–147	107.8–148.6	147
2	47.36							42–45	49.3–54.9	30
3	62.54–67.48	*c.* 57.32	70.16–70.68	43.88–46.52	51	45	54–66	45–65	44.5–67.9	60
4	47.86–50.72	*c.* 43.76	39.20–49.04	28.38–35.64	61	35	56–67	36–59	36.4–58.9	65
5	>150.06	>170.20	>191.05		167	127	175–190	130–176	125–195	>175
6	131.54								126.9–132.0	135.44[#]
7	156.12						149		152.5	152.08[#]
8		74.22						76	74.6–77.19	
9		28.26					35	31.5-35	25.8–31.8	
10		31.04							24.7–29.9	
11	85.52								89.1–101.7[*]	82.74[#]
12	105.94									105
13	67.78									72
14	110.52									131
15		*c.* 101.68			115	120	140		111.9–128.8	
16		31.52			39				22.3–26.3	
17		29.52					32		24.2–24.9	
18		40.04			48.5				41.8–48.5	
19		39.06							45.8–48.2	

Row numbers: Horncores = 1, width between the lateral sides at the base; 2, width between the internal sides at the base; 3, anteroposterior diameter at the base; 4, transversal diameter at the base; 5, length. Transversal diameter = 6, postorbital; 7, ectorbital-ectorbital; 8, between the external side of the occipital condyles; 9, the foramen magnum; 10, the occipital condyle; 11, skull behind the horncores, at the postcornual constriction; 12, palate on M3; 13, palate on P2; 14, face above the molar row; 15, occipitals. Height = 16, the occipital condyle; 17, the foramen magnum. Basioccipital = 18, transversal diameter of the caudal tuberosities; 19, transversal diameter of the rostral tuberosities. References: (1) Vislobokova et al. (1995); (2) Schaub (1923); (3) Bolomey (1965); (4) Duvernois and Guérin, 1989; (5) Crégut-Bonnoure (2025); (6) Teilhard de Chardin and Trassaert (1938). Some measurements from Schaub (1923) and Bolomey (1965) were re-measured by Crégut-Bonnoure (2025).
[*]Measurements from figs. 14.26–28 in Crégut-Bonnoure (2025); [#]measurements by the present authors.

Table 2. Measurements (in mm) of the upper cheek teeth of *Pliotragus* cf. *ardeus* from Xinyaozi and other related taxa.

	Pliotragus cf. *ardeus*	*Ovis zdanskyi*	*O. shantungensis*		*Pliotragus ardeus*				*Sinoryx bombifrons*	*Ovis* sp.
	V 31263.1	Anyang[1]	Shandong[2]	Nihewan[3]	Perrier[4]	Senèze[5]	Irimești[6]	Senèze and Dacian Basin[7]	Yushe Basin[8]	Udunga[9]
P2 L	14.22	13.59	9.9	6–7		15		12.9		
P2 W	13.26	12.63		8		13		11.7		
P3 L	16.28	16.62	11.5	10.5–11		11.5–13.5		15.3–16.5		
P3 W	16.16	16.16		11		15.5		14.3		
P4 L	14.89	14.54	11.5	11–11.5		12–14		13.4–16.8		10
P4 W	17.41	17.96		12.5		18		16.6–20.5		14
M1 L	18.36	18.43	21.5	19.5		15–20		15.5–18.1	14 (17.5)	22
M1 W	20.4	20.68		14		19–20		18.3–20.6	17 (16.5)	19
M2 L	22.58	21.86	27	21–22		17–22		19.9–24.1	20 (19.2)	23.5
M2 W	21.08	21.33		15–15.5		17–24		19.5–22.3	20 (20.3)	20
M3 L	24.9	25.32	30.5	24.5	22–25	22–31		19.7–31.5	25.5 (25.3)	
M3 W	22.46	20.14		15		15.5–22.5		18.9–23.1	19 (18.2)	
P2-4	44.39	44.79	35.2–35.5	30	29–39	43	43	51.3	47 (41.1)	
M1-3	64.46	66.43	74–74.9	64–65	60–62	62	71	62.5–64	68.2	62 (62.5)
P2-M3	106.56	108.1	105.7–116.0		89–91	106		102.5–105	119.3	(103.5)

References: (1) Bohlin (1938); (2) Matsumoto (1926); (3) Teilhard de Chardin and Piveteau (1930); (4) Depéret (1884); (5) Duvernois and Guérin (1989); (6) Bolomey (1965); (7) Crégut-Bonnoure (2025); (8) Teilhard de Chardin and Trassaert (1938); (9) Vislobokova et al. (1995). Measurements in brackets by the present authors.

basioccipital only exhibits weakly developed anterior basilar tuberosities, and the groove on the basioccipital is relatively deep. The palatine is flat and wide, with an oval palatal foramen located in between the M2 and M3. The distance between the palatal foramen and the palatal suture approximately equals that between the palatal suture and the lingual wall of M2/M3. The median palatal notch aligns approximately with the lateral palatal notch, extending anteriorly to the distal wall of M3.

Specimen V31264.1–3 is poorly preserved. V 31264.3 consists of a broken frontal with a well-separated pair of horncore bases (Fig. 3H). The horncores have a moderately round cross-section, and the frontal suture is slightly bulged in front of the horncores. V 31264.1, 2 are laterally compressed (Fig. 3A–G). The horncores are well preserved, tapering rapidly from base to tip. They are relatively straight at their base and in the middle portion, but slightly bent inward and backward at the distal end. Longitudinally developed grooves are present, more pronounced on the anterior surface than on the posterior one. The anterior rim of the horncore base is situated laterally, while the posterior rim is medially positioned on the skull, resulting in a convergent trend of the long axis of the horncore base from front to back. The horncores are located on the posterior rim of the orbit, without a postcornual pit at their bases. V 31264.1 retains a complete basioccipital (Fig. 3E). Its general outline resembles a rectangle, with the width of the anterior basilar tuberosities smaller than that of the posterior ones. The anterior basilar tuberosities are relatively flat, whereas the posterior ones are more developed. The groove between the basilar tuberosities is deep. The connection of left horncore and cranium in V 31264.2 may be repaired mistakenly. The main distinction between V 31264.1 and V 31264.2 is in the cross-section of the horncores: oval in V 31264.1 and more elongated anteroposteriorly in V 31264.2. All the measurements of the above-described skulls are listed in Table 1.

Upper cheek teeth. V 31263.1 contains a pair of complete upper cheek tooth rows (Fig. 2G). All teeth are mesodont. The tooth neck is bulged, different from hypsodont tooth of *Bos* and *Bison* which have a plane tooth neck. The ratio of upper premolar to molar row length is 0.69 in the left row and 0.67 in the right row. The occlusal outline of P2 appears irregular and semicircular, showing signs of significant wear, similar to that of the P2 in the holotype (Depéret, 1884, plate 8, fig. 3). The anterolabial cone is well developed, situated at the anterolabial aspect of the tooth. The anterolabial cone rib protrudes labially, and has the same level as the posterior style. The posterolabial cone is less distinct and merges with the posterior style through an indistinct

Table 3. Measurements (in mm) of the lower cheek teeth of *Pliotragus* cf. *ardeus* from Xinyaozi and other related taxa.

	Pliotragus cf. *ardeus*		*O. shantungensis*	*P. ardeus*			*Ovis* sp.
	V 31263.2	V 31263.3	Nihewan[(1)]	Senèze[(2,3)]	Dacian Basin[(4)]*	Senèze and Dacian Basin[(5)]	Udunga[(6)]
p2 L	11.56	10.42		10.5–11		9.9–12.5	
p2 W	8.7	6.04		5.5–7		5.6–8.3	
p3 L	13.04	13.74		12–13.5	13.8	13.0–15.1	
p3 W	11.33	9.49		9–11		7.6–10.7	
p4 L	16.98	17.39	12	15–18.5	16.2	16.1–18.5	20
p4 W	10.79	11.14	8	10.8–13		11.0–12.9	12
m1 L	16.96	17.16	16	17–18.5	17.3	16.1–21.9	
m1 W	14.59	13.96	10	12-15		13.0–15.1	
m2 L	20.24	20.8	22	18–23	20.2	18.7–23.6	25
m2 W	13.87	15.03	10	13.5–17		13.1–16.9	18.4
m3 L	30.04	29.62	28	28.5–36	29.2	30.3–34.6	
m3 W	13.99	13.32	10	11.5–15.5		12.1–15.0	
p2–4	41.79	41.92		44		42.8–44.6	
m1–3	67.9	69.12	66	79	77.5	71.4–71.8	66.8–83.4
p2–m3	110.16	112.52			106.2–114	128.4	

References: (1) Teilhard de Chardin and Piveteau (1930); (2) Depéret (1884); (3) Duvernois and Guérin (1989); (4) Croitor et al. (2024); (5) Crégut-Bonnoure (2025); (6) Vislobokova et al. (1995).
*Measured from figure.

posterolabial crista. The lingual cones of the right P2 consist of an anterolingual cone and a posterolingual cone, separated by a crista, while only one cone is present on the left P2. The posterolingual cone is wider than the anterolingual cone. The general outline of P3 is a more regular semicircular shape than that of P2. The anterolabial cone is prominent, while the posterolabial cone is weakly developed. Both the anterior and posterior styles are more developed compared to those of P2. The anterolabial cone rib is also developed as in P2; however, it is situated on the centre of the labial wall of the tooth, unlike the anterior situation of the rib in P2. The lingual cone of P3 is divided into an anterolingual cone and a posterolingual cone by a shallow groove on the lingual wall, and it is different from the P3 of the holotype which has no groove on the lingual wall. The anterolingual cone is more developed than the posterolingual cone. The outline of P4 resembles that of P3, with the buccal side dominated by the anterolabial cone. The anterolabial cone rib is not developed as that on P2 and P3. The anterior and posterior styles protrude buccally and are similarly developed to those of P3. Other structures of P4 closely resemble those of P3. The outline of M1 is nearly square, with the mesial lobe wider than the distal one. The parastyle and metastyle are weakly developed, while the mesostyle is highly pronounced. The paracone rib is more developed than the metacone rib. M2 and M3 exhibit a rectangular outline, sharing similar structures with M1. However, the parastyle and metastyle are more developed in M2–3, and the distal wall of M3 is moderately concave. The metastyle of left M3 is more developed than that of the right one, forming a wing shape in occlusal view. All upper molars feature enamel islets in the centre but lack any other accessory structures, similar to the molar teeth of extant Caprini. All the measurements of upper cheek teeth are listed in Table 2.

Lower cheek teeth. V 31263.2, 3 are two incomplete hemimandibles (Fig. 4A–F). V 31263.3 (Fig. 4D–F) exhibits the same level of wear as the upper cheek teeth (V 31263.1) mentioned earlier and fits well with the upper teeth, suggesting that they may belong to the same individual. There is a hole below the p3 of V 31263.2 (Fig. 4C), which is not the mental foramen, but might be a bite mark by Carnivora. All teeth on these two specimens are mesodont with a hypsodonty index of m3 (1.78) similar to that of extant *Tragelaphus imberbis* (1.91). The ratios of the lower premolar to molar row lengths are 0.62 for V 31263.2 and *c.* 0.61 for V 31263.3. The lower second premolar is only preserved on V 31263.2. The outline of p2 is plumped triangular. The anterior conid curves lingually, resulting in a shallow anterior valley. The mesolabial cone is prominent and conical, positioned in the middle labial aspect of the tooth. The mesolingual conid is not developed. The posterolingual conid protrudes lingually, making a relatively deep posterior valley. The morphology of p2 in lingual view is similar to the new specimens described by Crégut-Bonnoure (2025, fig. 14.31C). The outline of p3 is ladder-shaped. The morphology of the anterior half of p3 on V 31263.2 and 31263.3 is the same. The anterior stylid and anterior conid are less developed,

protruding lingually and separated by a shallow valley, similar to that from Senèze, France (Crégut-Bonnoure, 2025, fig. 14.31I). The mesolingual conid curves posteriorly. The anterior valley is 'V'-shaped in occlusal and lingual views. The posterior half of these two specimens is different, exhibiting a fused mesolingual conid and posterolingual conid with a shallow groove separating them in occlusal view on V 31263.3, and unfused on V 31263.2. Furthermore, the posterolingual conid protrudes more lingually than the mesolingual conid on V 31263.3. The posterior half of V 31263.2 and V 31263.3 is different from the specimen from Senèze described by Crégut-Bonnoure (2025, fig. 14.31I), which has an unfused mesolingual conid and posterolingual conid with the former protruding more lingually than the latter. The posterior half of p3 on V 31263.3 is similar to that of *Ovibos* and *Rupicapra*. Additionally, the posterolingual wall of the tooth inclines buccally, resulting in the distal half of the tooth being wider than the mesial half in described specimens. The outline of p4 is squared, and highly molarized, similar to the extant Caprini. A deep groove on the buccal surface of p4 divides the tooth into two lobes: the semicircular mesial lobe and the triangular distal lobe. The mesial lobe is larger than the distal one. The anterior stylid is less developed. The metaconid is elongated and rhombus-shaped, with a plump metaconid rib. The internal postmetacristid extends distally, touching the lingual wall of the entoconid but does not close the posterior valley in occlusal and lingual views. The distal lobe comprises a less-developed entoconid and a prominent hypoconid, both inclined buccally. They connect through the postentocristid and posthypocristid, and directly link with the internal postprotocristid via preentocristid and prehypocristid. The mesial part of the hypoconid is wider than the distal part. The posterior half of p4 is similar to NMB 562 (Crégut-Bonnoure, 2025, fig. 14.31F), but different from MNHN-F-1922-3 (Crégut-Bonnoure, 2025, fig. 14.31I) which has an entoconid and hypoconid arranged along the long axis of the mandible (NMB: Naturhistorische Museum Basel; MNHN: Muséum National d'Histoire Naturelle). General structures of the molars resemble those of the mesial lobe of p4. Stylids become more developed from m1 to m3. The anterior cingulid is weakly present on m2–3, displaying a small process in occlusal view, different from the specimens described by Crégut-Bonnoure (2025, fig. 14.31F,I) from Senèze. The third lobe of m3 on V 31263.2 is only dominated by a hypoconulid, whereas it consists of an unclear hypoconulid and entoconulid on V 31263.3. The third lobe of m3 inclines buccally, and is larger on V 31263.2 than on V 31263.3. A small cristid is present in the distal wall of the third lobe on V 31263.3, but absent on V 31263.2. The ectostylid is absent in V 31264.2, but developed in V 31264.3. All the measurements of lower cheek teeth are listed in Table 3.

Comparison and discussion

The specimens described in this article consist of three crania, one of which exhibits better preservation (V 31263.1) compared to the other two (V 31264.1, 2). V 31264.1 and V 31264.2 share several similarities, such as a slightly elongated braincase, straight horncore from proximal to middle parts, and gentle medial curvature towards the distal end, as well as the positioning of the horncores on the skull. Additionally, their similar surface colour suggests the same sedimentary environment. However, these two specimens differ in the cross-section of their horncores, with that of V 31264.1 displaying an elliptical cross-section (transversal diameter/anteroposterior diameter = 0.76), whereas that of V 31264.2 exhibits a more elongated oval one (transversal diameter/anteroposterior diameter = 0.56–0.69). Based on examination of the fracture surface of the horncore, we concluded that the horncores are well preserved without compression, despite the flattened nature of the crania. These differences in the cross-section morphology of the horncores indicates within-species variation. V 31263.1 shares some similarities in general morphology with V 31264.1, 2, such as the position of the horncores and the size of the braincase. Unfortunately, V 31264.1, 2 lack many morphological features for comparison. V 31264.3 is distinguished from the other crania by its round cross-section of horncores. This characteristic may indicate that it belonged to a juvenile individual given its smaller size. The two hemimandibles could be classified as the same species based on their similar morphology and size. Considering the above discussion, we conclude that the materials studied in this paper belong to the same species.

V 31263.1 shares with *Ovis zdanskyi* discovered in the Early Pleistocene deposits in Yangshao and described by Bohlin (1938) the compressed dorsoventrally cranial shape, the relatively wide muzzle, the relatively large preorbital fossa, and the similarly developed basilar tuberosities (Fig. 5). However, obvious differences exist in horncore morphology and teeth measurements. The horncore of *O. zdanskyi* is curved posteriorly with a triangular cross-section, similar to extant male *Ovis ammon*. It differs from our specimens, which have a relatively straight horncore with an oval cross-section (Fig. 5). The tooth measurements are also different between *O. zdanskyi* and our specimens, with

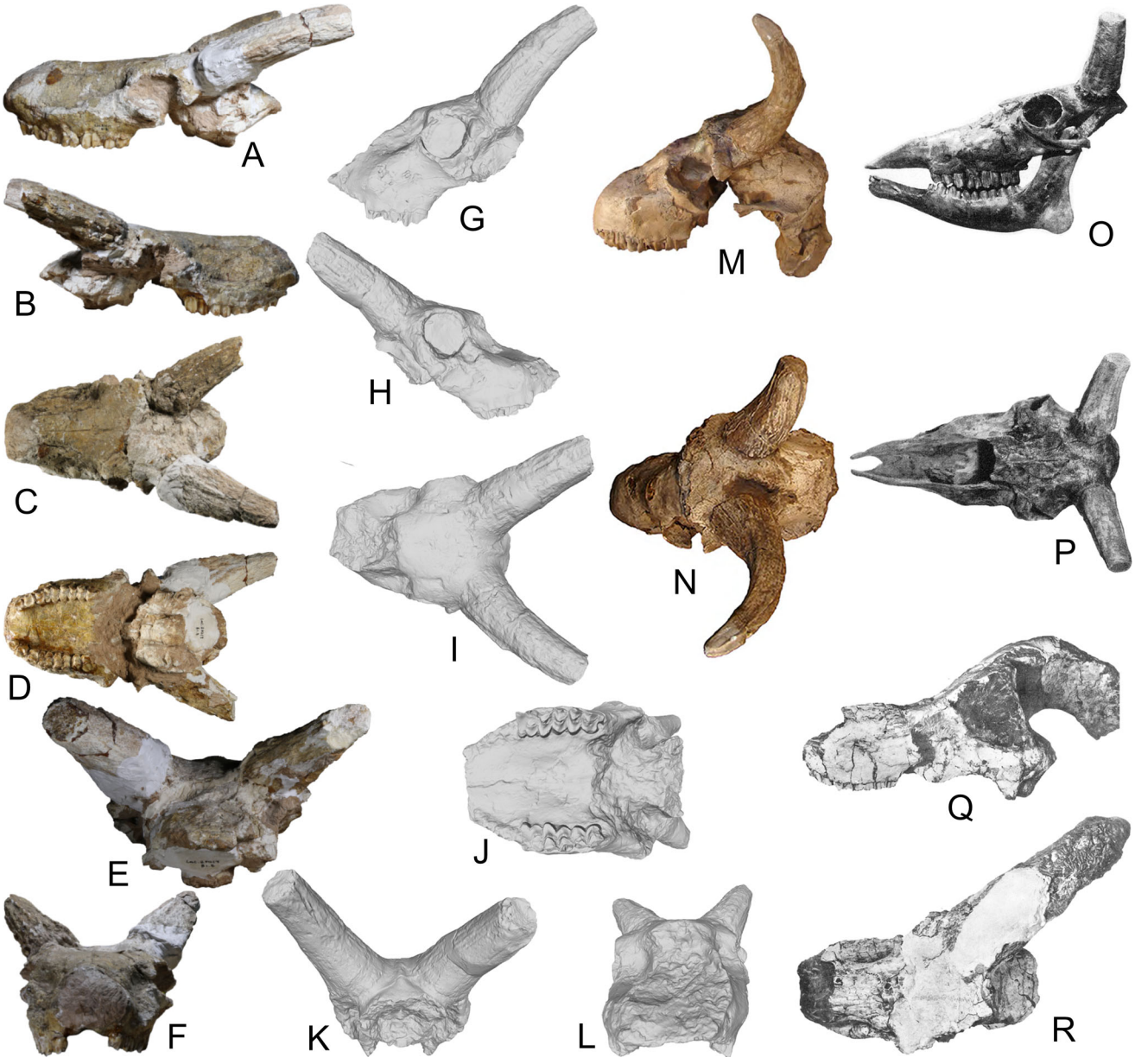

Figure 5. A well-preserved skull of *Pliotragus* cf. *ardeus* (V 31263.1) from Xinyaozi (**A**–**F**) and the skulls of other Caprini (**G**–**R**). **G**–**L,** *Sinoryx bombifrons* (Teilhard de Chardin & Trassaert, 1938); **M, N,** *Hesperidoceras merlae* (Rodrigo, 2011); **O, P,** *Megalovis latifrons* (Schaub, 1943); **Q, R,** *Ovis zdanskyi* (Bohlin, 1938). **A, G, M, O, Q,** left lateral views; **B, H,** right lateral views; **C, I, N, P, R,** dorsal views; **D, G,** ventral views; **E, K,** posterior views; **F, L,** anterior views. Images not shown to scale.

O. zdanskyi having a shorter upper premolar row (premolar length/molar length = 0.47–0.48) than that of our specimens (premolar length/molar length = 0.67–0.69) (Fig. 6B, Table 2; Supplemental material Table S2). Although extant *Ovis* show strong sexual dimorphism with the female having smaller and relatively straighter horncores than the male, several dissimilar characteristics, such as the anteroposterior axis of the cross-section of the horncores being parallel or inclined to the sagittal plane in female *Ovis* but inclined outward in our specimens, suggest that they likely represent distinct species.

Northern China has revealed a diverse group of *Protoryx* described by Bohlin (1935) and Teilhard de Chardin and Trassaert (1938), including five distinct taxa: *P. plantifrons*, *P. shansiensis*, *P. yushensis*, *P. bohlini* and *Protoryx* sp., discovered in Upper Miocene to Lower Pliocene deposits. Later, these species were reclassified into two new genera,

Huabeitragus and *Macrotragus*, by Chen and Zhang (2007). Compared with these two genera, the Xinyaozi specimens are distinct due to their less divergent and more strongly inclined horncores, larger distance between the horncore bases, greater distance between the horncore and orbit, and a larger angle between the facial and cranial axis. Additionally, both *Huabeitragus* and *Macrotragus* were discovered in the Late Miocene to Early Pliocene, predating the Xinyaozi specimens.

Compared with *Euceratherium* sp. discovered in the same locality (Bai, Dong, et al., 2024), our specimens differ in their smaller teeth and shorter tooth row (Figs 6B, 7; Supplemental material Tables S2–S4). Additionally, stylids on the teeth of *Euceratherium* sp. are more developed than those of the current specimens.

Based on comparisons with other Caprini, we observed that the Xinyaozi specimens show a striking resemblance to *Pliotragus ardeus*, which was predominantly found in Europe and recently reviewed by Crégut-Bonnoure (2025). The horncores of crania studied herein share some similarities with NMB Se 1636 from Senèze, France (Crégut-Bonnoure, 2025; Schaub, 1923) and Gr. 454/207 (Gr: Grăunceanu) from Irimești, Romania (Bolomey, 1965), exhibiting a rough surface, the same internal distance between basal horncores (NMB Se 1636: 49.3 mm; Gr. 454/207: 40 mm; V 31263.1: 47.36 mm), a similar angle of the horncores (V 31263.1: *c.* 55°; NMB Se 1636: *c.* 60°, see Schaub [1923, fig. 3]; Gr. 454/207: *c.* 70°, see Bolomey [1965]), rapid tapering from base to tip, slight medial curvature at the distal end, and similar positioning relative to the orbit. However, V 31263.1 differs from MNHN-F-1923-8 by the horncores curving posteriorly in lateral view and the smaller angle of the horncores (*c.* 55°), whereas the horncores are directed forward and the angle of the horncores is larger (*c.* 120°) in MNHN-F-1923-8 (Crégut-Bonnoure, 2025). V 31264.1 is also different from an unnumbered specimen unearthed from the Dacian Basin, Romania by the larger angle of horncores in the latter specimen (*c.* 95°) (Crégut-Bonnoure, 2025). Furthermore, the horncore measurements of the European material are variable, particularly in their anteroposterior and transversal diameters (Fig. 6A; Supplemental material Table S1).

Although Croitor et al. (2024) classified the European discovered horncore into two sexes based on size, specimens within the same gender still exhibit two morphologies: equal anteroposterior-transversal diameters and anteroposterior diameter larger than transversal diameter. Based on our examination of horncore illustrations by previous researchers, we concluded that the cross-section morphology of the horncores in *P. ardeus* is variable (Fig. 6A; Supplemental material Table S1). This assertion is also supported by the observation of a slight medial curvature in the horncore as depicted by Schaub (1923) and Crégut-Bonnoure (2025) (NMB Se 1636), a moderate curvature in the illustrations by Bolomey (1965) (Gr. 454/207), and a pronounced curvature in those by Duvernois and Guérin (1989) and Crégut-Bonnoure (2025) (MNHN-F-1923-8). Hence, other disparities between our specimens and the aforementioned materials, such as the absence of a crest on the posterior side of the horncore and more pronounced grooves on the anterior side, may be attributed to intraspecific variation. The cranium of the Xinyaozi specimens bears resemblance to the crania unearthed from Senèze (Crégut-Bonnoure, 2025; Duvernois & Guérin, 1989; Rodrigo, 2011; Schaub, 1923) and Irimești

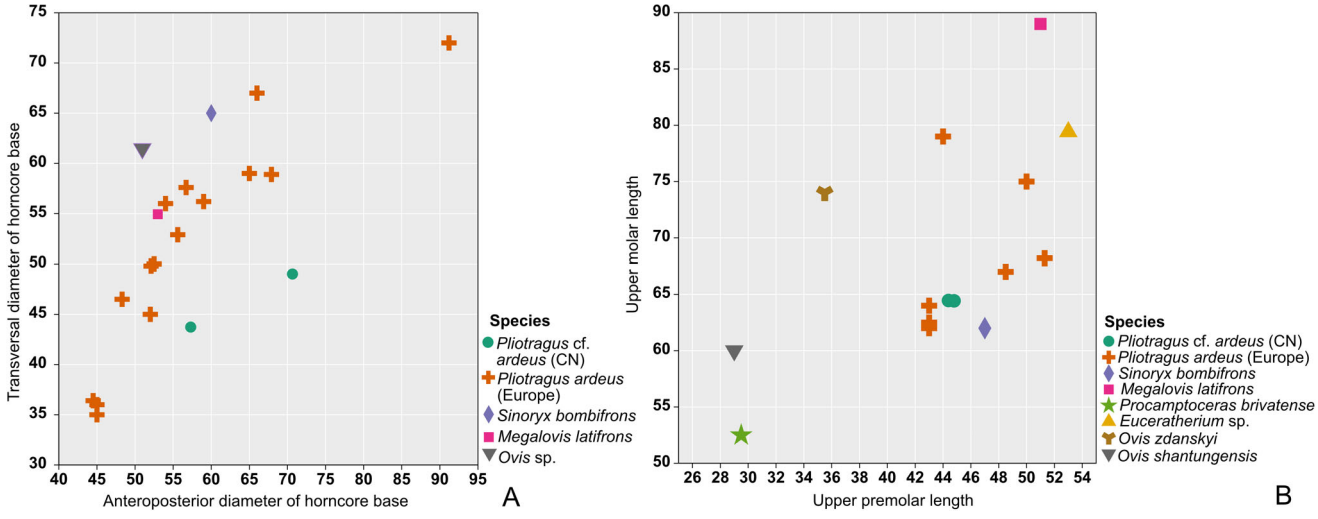

Figure 6. Plots of **A,** basal horncore diameters and **B,** upper cheek teeth length of *Pliotragus* cf. *ardeus* from Xinyaozi and other related taxa. Data from: Bolomey (1965); Croitor et al. (2024); Depéret (1884); Duvernois & Guérin (1989); Teilhard de Chardin and Trassaert (1938); Schaub (1923), Crégut-Bonnoure (2025). See also Supplemental material Tables S1, S2.

(Bolomey, 1965), characterized by a small supraorbital foramen, large preorbital fossa, anterior rim of orbits positioned atop of M3, relatively elongated braincase, occipital bulging posteriorly, and a rectangular basiooccipital with relatively developed basilar tuberosities. Furthermore, the cranial measurements between European and our specimens are similar (Table 1).

Comparatively, the upper cheek teeth of V 31263.1 share similar measurements (Fig. 6B; Table 2; Supplemental material Table S2) and characteristics with those from Perrier-Etouaires (Depéret, 1884) and Irimești (Bolomey, 1965). For instance, the groove on the lingual wall of the upper premolar is subtle, and the ratio between upper premolar and molar row (0.69 mm and 0.67 mm in Xinyaozi, 0.69 mm in Perrier-Etouaires, and 0.67–0.69 mm in Irimești), as well as the total upper cheek teeth row length (106.56 mm and 108.1 mm in Xinyaozi, 106 mm in Perrier-Etouaires, and 102.5–104 mm in Irimești) are similar. However, the upper cheek teeth of V 31263.1 are smaller than those of the new specimen described and measured by Crégut-Bonnoure (2025) (Xinyaozi: upper premolar, 44.39–44.79 mm; upper molar, 64.46–66.43 mm. Senèze: upper premolar, 51.3 mm; upper molar, 68.2 mm), and exhibit a different upper premolar to upper molar ratio (Xinyaozi: 0.67–0.69 mm; Senèze: 0.75 mm). The lower cheek teeth in Xinyaozi resemble those of *P. ardeus* discovered from Senèze (Crégut-Bonnoure, 2025) and the Dacian Basin (Croitor et al., 2024) in their measurements (Table 3; Supplemental material Tables S3, S4) and morphologies, for instance, the mesolingual conid extending posteriorly and closing the posterior valley and back valley in p3, and high molarization of p4. The logarithmic ratio diagrams with error bar of the upper and lower cheek teeth also indicate that our specimens are located within the known variation of *P. ardeus* (Fig. 7). However, it is important to note that the tooth sizes in the specimens from Senèze are variable (Tables 2, 3), likely due to different degrees of tooth wear. Besides that, the morphology of the tooth is also variable; for instance, the ectostylid is absent in NMB Se 562, but is very developed in MNHN-F-1922-3. Similarly, the ectostylid is absent in V 31264.2 but developed in V 31263.3. In summary, the resemblance observed between the caprine bovid from Xinyaozi and the European *Pliotragus ardeus* warrants the classification of the Chinese archaic caprine from Xinyaozi as *Pliotragus* cf. *ardeus*.

Most previous reports of *Pliotragus* findings have emanated from Europe, except for some isolated teeth discovered in Turkey (western Asia) and classified as

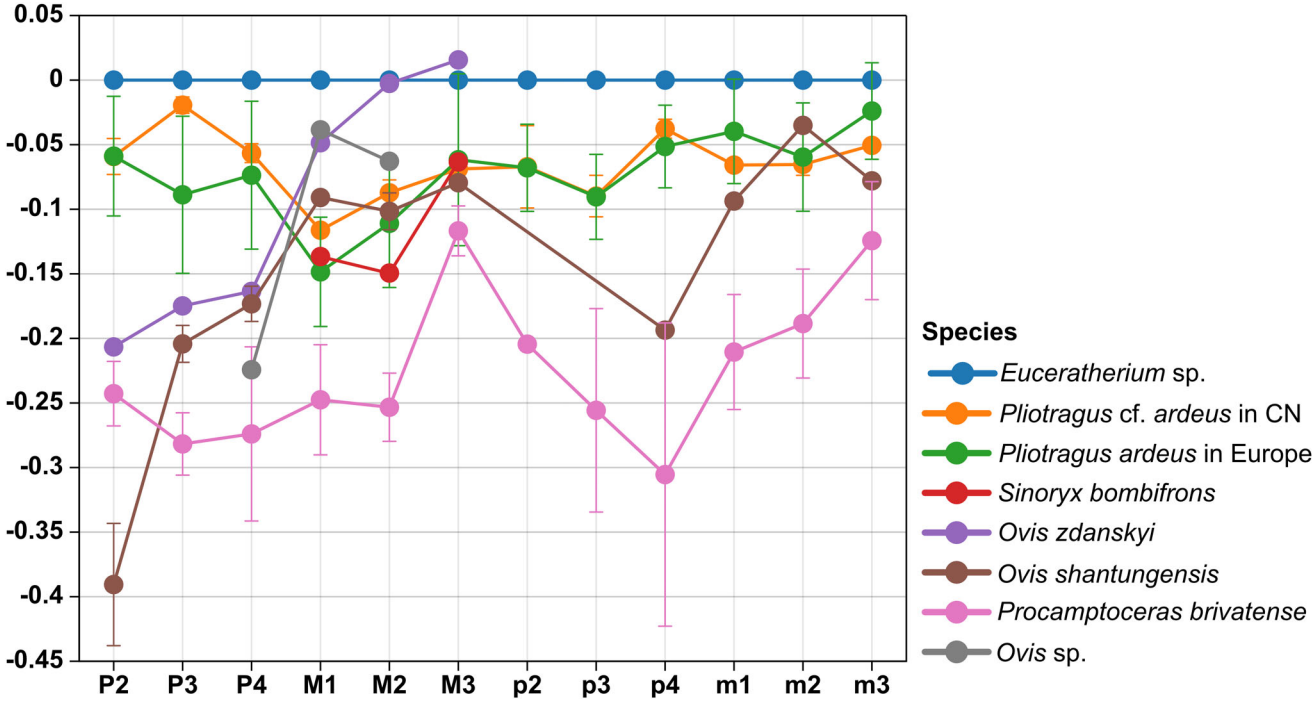

Figure 7. Simpson's logarithmic ratio diagram of upper and lower cheek teeth length of *Pliotragus* cf. *ardeus* from Xinyaozi and other related taxa. Data from: Matsumoto (1926); Bohlin (1938); Croitor et al. (2024); Duvernois and Guérin (1989); Teilhard de Chardin and Piveteau (1930); Teilhard de Chardin and Trassaert (1938); Vislobokova et al. (1995); Bai, Dong, et al. (2024); Crégut-Bonnoure (2025). See also Supplemental material Tables S3, S4.

cf. *Pliotragus* (Kostopoulos & Sen, 1999). In addition, Gentry (2001) described a frontal bone with a horncore and cranial roof unearthed from an unknown layer in Austria, classifying this material as *Pliotragus* sp. This specimen shares similarities with *P. ardeus*, notably featuring a triangular-shaped horn core base and the position of the horncore on the frontal bone. However, a distinction lies in the fact that the horncore of the Austrian specimen is straight from base to tip, unlike the medial bending at the distal part of the horn core in *P. ardeus*. The Austrian material is incompletely preserved, and its classification warrants further discussion in the future. Another species, *P. macedonicus*, was discovered in early Middle Pleistocene deposits in Northern Greece, represented by several upper molars (Crégut-Bonnoure & Tsoukala, 2005).

Some bovid finds from eastern Asia bear a resemblance to *Pliotragus* specimens (V 31263.1) from Xinyaozi, especially *Sinoryx bombifrons* from the Yushe Basin, described by Teilhard de Chardin and Trassaert (1938) based on an incomplete skull with upper molars. Similarities include measurements of the tooth row and cranium (Fig. 6B, 7; Tables 1, 2; Supplemental material Tables S2–S4) (It is worth noting that the length of M1 measured by Teilhard de Chardin and Trassaert [1938] was 14 mm, but re-measured by the present authors as *c.* 17.5 mm at alveoli based on the cast of this specimen. The ratio of re-measured upper premolar to upper molar length in Xinyaozi [0.67–0.69] is similar to that of *S. bombifrons* [0.66)] and some cranial characteristics, such as the medially bending horncore at its distal portion, several grooves on the horncores, large preorbital fossa, broad muzzle, and the position of the horncore relative to the orbit. However, the horncores of V 31263.1 differ from *S. bombifrons* in their oval cross-section, the larger distance between the horncore bases (this difference may be influenced by the individual variation and cranial dorsoventral compression). V 31264.3 exhibits a closer resemblance to *S. bombifrons* due to its rounded cross-section of the horncore; however, its poor preservation prevents a detailed comparison. Likewise, *S. bombifrons* is similar to *P. ardeus* from Europe with respect to the size of the cranium and upper teeth (Tables 1, 2) (upper premolar length/upper molar length, *S. bombifrons*: 0.66; Senèze: 0.67–0.75), and some cranial and horncore characteristics, such as medially convergent horncore, large preorbital fossa, and the position of the horncore relative to the orbit. It seems that *Pliotragus ardeus* is probably a junior synonym of *S. bombifrons* because the latter name was erected by Teilhard de Chardin and Trassaert (1938) and therefore has priority over Kretzoi (1941) based on the International Code of Zoological Nomenclature. Remains of *S. bombifrons* were unearthed from the deposits in Zhangwagou, Yushe Basin (pers. comm. with Prof. Shiqi Wang from IVPP, 2 December 2024), which was magnetostratigraphically dated to *c.* 3.3–3.0 Ma (Opdyke et al., 2013), predating the Xinyaozi and Europe material. Although a broken skull reported as *S. bombifrons* was discovered in Early Pleistocene deposits of Tuozidong Cave (Fang et al., 2004), this material is fairly incomplete, lacking preservation of the facial part and horncore, making its taxonomic classification uncertain. Whether these two taxa are synonyms still needs to be further investigated.

Another intriguing bovid was described by Vislobokova et al. (1995) as *Ovis* sp. from Late Pliocene deposits in Udunga, Russia. The Udunga material comprises a neurocranial fragment, horncore, limb bones, and some isolated teeth. Ogino et al. (2009) suggested that these remains should be attributed to *Gazella*. The Udunga specimens exhibit significant similarities to those from Xinyaozi in terms of the developed grooves on the anterior side of the horncore, as well as the outline of the basioccipital and the morphology of p4. Additionally, the Udunga material bears resemblance to *Pliotragus ardeus* from Valea Grăunceanului: the neurocranial fragment from Udunga (with a greatest occipital width of 115 mm) is only slightly smaller than the male neurocranium from Valea Grăunceanului (with an occipital width of 120 mm re-measured by Crégut-Bonnoure, 2025). Measurements of the horncore from Udunga are similar to those from Valea Grăunceanului (Fig. 6A; Supplemental material Table S1). However, the horncore from Udunga appears to be straighter compared to the specimens from Xinyaozi and Europe, and there are differences in the size of the upper premolar teeth as well (Table 2, Fig. 7). Moreover, in comparison to horn cores of *P. ardeus* from Romania (Croitor et al., 2024), the horn core from Udunga is also relatively straighter and slenderer, while its pedicle is less distinguishable than in Romanian specimens. Hence, the bovid from Udunga might represent a distinct species. Further investigation is necessary to ascertain the taxonomic classification of the Udunga specimens. Nevertheless, it is evident that they cannot belong to *Gazella* (*s. l.*) due to the relatively large size of the horncore and other morphological differences.

Taxonomy and systematic position of *Pliotragus ardeus*

The taxonomic diversity within the genus *Pliotragus*, as well as its systematic position, remain unresolved. The primary reason for these unresolved questions is the scarcity of available fossil material, which hinders

understanding of intraspecific morphological variation and taxonomically significant characteristics. This scarcity also complicates the identification of evolutionary specializations of *Pliotragus ardeus*, making it difficult to determine its affinities with other bovid phylogenetic lineages (Bolomey, 1965; Crégut-Bonnoure, 2007; Croitor et al., 2024; Duvernois & Guérin, 1989; Gentry, 2001; Kostopoulos & Sen, 1999; Schaub, 1923; Schaub, 1943). Currently, there are reports of several poorly known forms tentatively ascribed to the genus *Pliotragus* and two species: *P. ardeus* (Depéret, 1884) from the Villafranchian of France, Spain, and Romania; and *P. macedonicus* Crégut-Bonnoure and Tsoukala, 2005 from the early Middle Pleistocene of Greece. However, according to Kostopoulos (2022), the validity of the latter species needs to be confirmed due to the limited material (three isolated teeth).

The initial allocation of this bovid in the genus *Antilope* by Depéret (1884) was rather arbitrary since the available material was incomplete. Schaub (1923) considered the systematic position of the genus as rather uncertain. Kretzoi (1941) replaced the genus *Deperetia* Schaub, 1923 with *Pliotragus*. This taxonomic revision is currently unanimously accepted (Crégut-Bonnoure, 2025; Crégut-Bonnoure & Tsoukala, 2005; Croitor et al., 2024; Duvernois & Guérin, 1989; Kostopoulos, 2022; Sokolov, 1953). Sokolov (1953) published an overview of the craniodental morphology of *Pliotragus*, which was then regarded as Bovidae *incertae sedis*. Some statements from Sokolov (1953) are mistaken, possibly leading to his inability to determine the systematic position of *Pliotragus*. For instance, Sokolov (1953) asserted that the horncores in *Pliotragus* are situated immediately above the orbits. However, subsequent examinations of *Pliotragus* cranial material have shown that the horncores are clearly positioned caudally relative to the orbits (Bolomey, 1965; Crégut-Bonnoure, 2025). Additionally, Sokolov (1953) claimed that *Pliotragus* is characterized by pneumatization of frontal bone, whereas the horncores are practically non-pneumatized, with only their pedicles being hollowed. This contradicts the findings of Croitor et al. (2024), who studied a series of *Pliotragus* horncores from southern Romania and reported that at least the proximal part of the horncores is pneumatized. Viret (1961) also classified *Pliotragus* as *incertae sedis*. Guérin (1965) referred to *Pliotragus* (as *Deperetia*) as a genus *incertae sedis*, which is supposedly close to *Rupicapra* (and some fossil relatives). Guérin (1965) further suggested a close relationship between *Pliotragus ardeus* and *Hesperidoceras merlae* from the Villafranchian of Villaroya (Spain).

Gentry (1970, 1971) proposed that *Pliotragus* might be a synonym of *Megalovis*, basing this assumption on a comparison of limited *Pliotragus* cranial material with the type skull of *Megalovis latifrons* from Senèze, which might belong to a female. The cranial morphology of *Megalovis latifrons* exhibits pronounced sexual dimorphism, and the holotype of *M. latifrons* should be female (Crégut-Bonnoure & Dmitrijevic, 2006; Croitor et al., 2024). Consequently, Gentry (1970, 1971) arrived at a mistaken conclusion if the statements of Crégut-Bonnoure and Dmitrijevic (2006) and Croitor et al. (2024) are correct, since male cranial material of *Megalovis latifrons* was unknown at that time. Later, Gentry (2001) mentioned *Pliotragus ardeus* and *Megalovis latifrons* as two distinct species in different genera, but he did not exclude the possibility of synonymy between them. Hitherto, these two species are still regarded as different genera (Crégut-Bonnoure, 2025; Duvernois & Guérin, 1989) based on the clearly different morphologies of their horncores. Gentry (1971) suggested that the skull shape of *Pliotragus*, as figured by Bolomey (1965), indicates a connection with *Paleoryx pallasi*, aligning with an earlier assumption proposed by Schaub (1923). According to Gentry (1971), the systematic position of *Paleoryx* is ambiguous: it could be placed in the tribe Caprini together with *Pachytragus crassicornis* (this species has been reclassified as *Protoryx capricornis* by Kostopoulos, 2009), or have a closer relationship to *Ovibos* (and other fossil relatives). Despite doubts raised by Gentry (2001) about the validity of *Pliotragus*, he consistently maintained that *P. ardeus* should be close to *Ovibos* (and other fossil relatives).

Gentry (1971) proposed that *Sinoryx bombifrons* and *Paleoryx sinensis* also belong to the early evolutionary radiation of *Ovibos* (and other fossil relatives). In our opinion, *Sinoryx bombifrons*, established by Teilhard de Chardin and Trassaert (1938), bears significant resemblance to *P. ardeus* in terms of the general outline of the horncores, large preorbital fossa, and other skull and teeth measurements (Tables 1, 2), suggesting that this species may be ancestral to or a synonym of *P. ardeus*. Its rounded horncore cross-section is reminiscent of the morphological variant of *P. ardeus* described from Valea Grăunceanului (Croitor et al., 2024) and Senèze (Crégut-Bonnoure, 2025).

Duvernois and Guérin (1989) suggested that *P. ardeus* is an intermediate form between *Rupicapra* (and other fossil relatives) and *Ovibos* (and other fossil relatives), and closer to the latter based on its dental morphology. They included *Hesperoceras merlae* (*nomen nudum*? replaced by *Hesperidoceras merlae*) from the Villafranchian of Villaroya (Spain) in the synonymy list of *Pliotragus ardeus*, noting that the two species are practically identical. However, Duvernois and Guérin (1989) acknowledged that the Spanish bovid was distinguished by the anterior bending of the distal parts of the horncores. Rodrigo (2011) provided a detailed morphological comparison of Spanish and

French material, describing a series of morphological features that distinguish these two rarely reported species. This study revealed that the cranial morphology of *Hesperidorceras merlae* and *Pliotragus ardeus* is quite different, particularly the horncores and basioccipital (Rodrigo, 2011, fig. 5.1, plate 22). Additionally, the relatively short orbitofrontal portion of the skull in the Spanish bovid is noteworthy; the anterior edge of the orbit is situated above M3 (Rodrigo, 2011), whereas in *P. ardeus* from Romania, the anterior edge of the orbit is situated behind M3 or at the same level as the posterior wall of M3 (Bolomey, 1965). Furthermore, the occipitoparietal angle in *Pliotragus* is very obtuse, while that in *Hesperidoceras* approaches 90°. The shape of the metacarpals in *H. merlae* is also clearly different from *P. ardeus*, being more robust. Therefore, we conclude that *H. merlae* is a distinct species. According to the dendrogram based on horncore and cranial roof characteristics published by Gentry (2001), *Hesperidoceras* and *Pliotragus* are clustered individually with other fossil taxa as two different clades. Crégut-Bonnoure (2007) considered that *Pliotragus* should be close to *Rupicapra* (and other fossil relatives); however, she did not provide supporting arguments for this classification.

As a result, two hypotheses have been proposed regarding the tribal affiliation of *P. ardeus*, suggesting it belongs either to Antilopini or Caprini (*Ovibos* [and other fossil relatives] or *Rupicapra* [and other fossil relatives]). Compared to typical Antilopini, *P. ardeus* exhibits several distinguishing characteristics, such as pneumatized horn cores, a larger body size, a small supraorbital foramen, the absence of a postcornual pit, and the short distance between the horncore base and the orbital rim. Consequently, *P. ardeus* should not be placed in Antilopini.

Although Gentry (2001) considered that *P. ardeus* should have a closer relationship to *Ovibos* (and other fossil relatives), the phylogenetic analysis performed by him only included *Ovibos* and other fossil relatives without adding any other bovid groups in this analysis. Therefore, the result might be biased. In addition, the species differs from *Ovibos* (and other fossil relatives) by its longer skull at the postcornual part, with the horncore extending posteriorly instead of bending anteriorly as in *Ovibos* (and other fossil relatives). We consider that this species may not belong to the clade of *Ovibos* and other fossil relatives. The last consideration of closer relationships to *Rupicapra* is still questionable because the horncores of *Pliotragus* grew laterally and are oval or triangular in cross-section, unlike in *Rupicapra* where the horncores grew parallel to each other and are round in cross-section. This taxonomic consideration may be influenced by the first detailed description of the horncore by Schaub (1923, p. 289) as "its horncore is similar to *Antilocapra*", which has a similar horncore morphology to *Rupicapra*.

In order to determine the phylogenetic relationships of *Pliotragus* cf. *ardeus* (Xinyaozi) and *Pliotragus ardeus* (Europe) with other bovids, we assembled a matrix of molecular characters (Hassanin et al., 2012) and morphological characters (Bärmann, 2012; Wang et al., 2023; according to the descriptions and illustrations from Bolomey, 1965; Croitor et al., 2024; Depéret, 1884; Duvernois & Guérin, 1989; Schaub, 1923; Crégut-Bonnoure, 2025), and performed a Bayesian total-evidence dating analysis (see Bai et al., 2025 for phylogenetic data). The results of this Bayesian analysis reached convergence. In our 50% majority-rule consensus tree (Fig. 8), *Pliotragus* cf. *ardeus* (CN), *P. ardeus* (Europe) and *Sinoryx bombifrons* form a clade. They are positioned in Caprini, as the sister group of the clade of *Capricornis crispus-Ovibos moschatus-Euceratherium collinum*. Our analysis indicates that *P. ardeus* might have a closer relationship with *Ovibos* than *Rupicapra*; however, it should be a stem group of the clade of *Capricornis crispus-Ovibos moschatus-Euceratherium collinum*, representing an early evolutionary stage of this clade. In addition, the sister group relationship between *P. ardeus* and *S. bombifrons* suggests that they might have a closer relationship. Based on the morphological matrix (see Bai et al., 2025 for phylogenetic data), we can see that the main differences among *Pliotragus* cf. *ardeus* (CN), *P. ardeus* (Europe) and *S. bombifrons* are: the posterior end of the upper tooth row at the anterior margin of the orbit in *P. ardeus* (Europe), whereas these are below the orbit in *S. bombifrons* and *Pliotragus* cf. *ardeus* (CN); the third lobe of m3 in *Pliotragus* cf. *ardeus* (CN) consists of hypoconulid and entoconulid or hypoconulid only, but only consists of hypoconulid in *P. ardeus* (Europe); the cross-section of the basal horncore is variable in *P. ardeus* with both round and oval shapes, but only has a round or oval shape in *S. bombifrons* and *Pliotragus* cf. *ardeus* (CN). The first character cannot be obviously defined because the orbit of *S. bombifrons* and *Pliotragus* cf. *ardeus* (CN) is only located on top of the distal lobe of M3, closer to that of *P. ardeus* (Europe) being in the same line with the posterior margin of the upper tooth row; the second character indicates that it is probably variable in *Pliotragus* cf. *ardeus* (CN); the last character is variable and cannot distinguish *Pliotragus* and *Sinoryx*. Therefore, we consider that *Pliotragus* and *Sinoryx* might be synonymous based on their similar morphology and size. However, this hypothesis still needs to be verified after more complete material has been discovered and systematically studied.

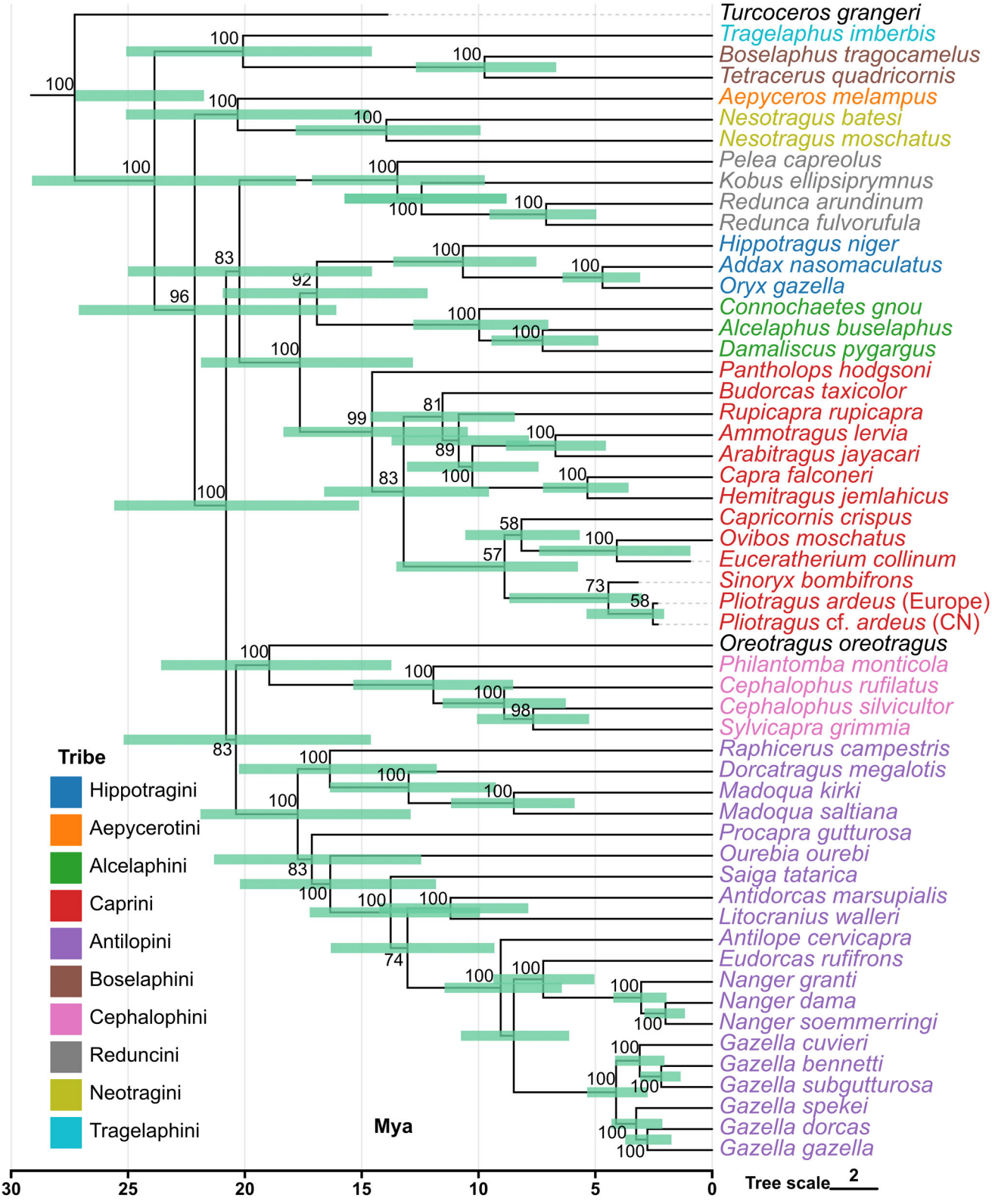

Figure 8. Phylogenetic position of *Pliotragus ardeus* within extant Bovidae, with *Turcocerus grangeri* as the outgroup. 50% majority-rule consensus tree resulting from a Bayesian total-evidence dating analysis using MrBayes 3.2.7 (see Bai et al., 2025 for phylogenetic data). The numbers on each node are the posterior probabilities, and the node bars are 95% confidence age intervals. The figure was generated according to Xie et al. (2023).

Palaeodiet and palaeohabitat of *Pliotragus ardeus* and the palaeoclimatological implications

The diet and habitat of *Pliotragus ardeus* is poorly known. This species is one of the largest forms in Caprini, and does not exhibit the typical morphology of taxa that lived in mountain habitats, such as goats. Croitor et al. (2024) proposed that *Pliotragus ardeus* exhibited adaptations for cursorial locomotion, superimposed on initial specializations characteristic of a mountain climber. It represents an early form that shifted habitats from mountains to plains driven by mid-Pliocene climate cooling (Croitor et al., 2024). However, aside from the discussion in Croitor et al. (2024), no studies have focused on the habitat of this species.

To investigate the diet of *Pliotragus* cf. *ardeus* discovered from Xinyaozi and *Pliotragus ardeus* from Europe, we plotted the ratio of lower premolar length to lower molar length and hypsodonty index of *Pliotragus* (Xinyaozi and Europe) and other extant bovids provided by Mendoza et al. (2002) (Fig. 9) (see also Supplemental material Table S5). The results show that the categories of GBr and CMf are distinct from the categories of GGr, FGr and OMf, although some taxa (i.e. *Pelea capreolus* and *Raphicerus melanotis*) influence the differentiation of these two dietary categories, giving them a large overlap. We considered that these divisions can be used as an appropriate approximation for the ecology of bovids as suggested by Mendoza et al. (2002). Therefore, the position of our specimen in between the GBr and CMf groups indicates its probable

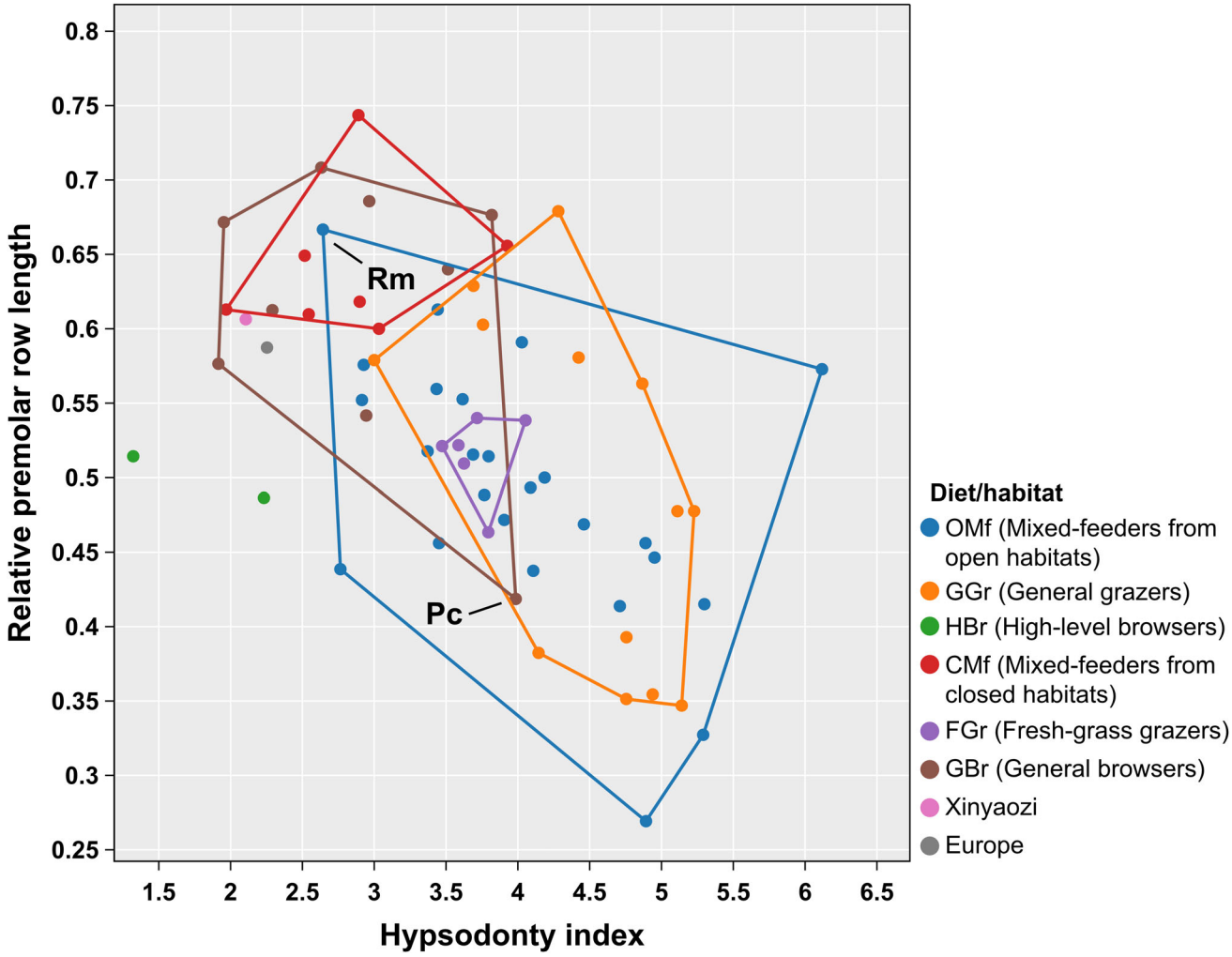

Figure 9. Relative length of the lower premolar tooth row ([length P2–P4/length M1–M3]×100) and hypsodonty index ([unworn M3 crown height/average width]×100) of *Pliotragus* cf. *ardeus* from Xinyaozi and *P. ardeus* from Europe (Crégut-Bonnoure, 2025) compared with modern bovids (data from Mendoza et al., 2002). The total height of m3 of the Xinyaozi specimen is estimated. **Abbreviations: Pc**, *Pelea capreolus*; **Rm**, *Raphicerus melanotis*. See also Supplemental material Table S5.

dominant browsing habitat, with it consuming more leaves than grass (Fig. 9). We also plotted the mean values of the data of the European samples provided by Crégut-Bonnoure (2025) on the same diagram. European *P. ardeus* is located in GBr, indicating a dominantly browsing habitat. Additionally, the tooth crowns of *P. ardeus* are significantly lower than those of typical grazers, as indicated by the wider teeth necks (Depéret, 1884, plate VIII, fig. 3; Duvernois & Guérin, 1989, plate III, fig. 1).

To further estimate the dietary preferences of this species, a mesowear analysis was performed according to the dataset established by Carranza-Castañeda and Jiménez-Hidalgo (2021). Based on the scoring system created by Fortelius and Solounias (2000) and improved by Fraser et al. (2014), we scored m2 100% (N = 2) high cusp and 100% (N = 2) round cusp for the Xinyaozi specimen and 100% (N = 6) high cusp, 33.3% (N = 2) sharp cusp, 33.4% (N = 2) round cusp and 33.3% (N = 2) really round cusp for the European specimens (sharp cusp: NMB Se 562, MNHN-F-1922-3; round cusp: NMB Se 1459, NMB Se 1719; really round: NMB Se 383, NMB Se 1733 [Crégut-Bonnoure, 2025]) (see Supplemental material Table S6), and conducted a hierarchical cluster analysis and a discriminant function analysis (DFA). The results of the hierarchical cluster analysis show that grazers and browsers can be clearly distinguished because of their bifurcation at the tree root (Fig. 10A). The Xinyaozi and European specimens are clustered with a clade of browsers (Fig. 10A). In addition, the DFA of the same dataset resulted in two canonical discriminant functions, the first of which has statistical significance ($p < 0.001$, Wilks' lambda), and contributes to 92.7% of the variance. The percentage of individuals with high cusp has the greatest influence on the function (loading = –0.692). The percentage of individuals with sharp and round-blunt cusp have nearly as large influence as that of high cusp on the function (loading: –0.552; 0.492). The DFA could classify 83.9% of the dataset correctly according to the mesowear scoring. The misclassifications include browsers classified as mixed-feeders classified as browsers and grazers. No grazers or browsers are mistakenly classified as each other. Based on the results of this analysis, the European and Chinese *Pliotragus* have a closer distance to the group centroid of browsers. Based on the significance of DF1, the European *Pliotragus* appears closer to mixed-feeders. Although the sample size of Chinese *Pliotragus* is small and it might not be plotted on the diagram precisely, the diet of Chinese *Pliotragus* should be browser or mixed-feeder. In summary, *P. ardeus* should be a browser or mixed-feeder.

In order to investigate the habitat of *P. ardeus*, we performed a PCA based on the measurements of metacarpal and radius of *P. ardeus* and other bovids of known ecomorphology (see Supplemental material Tables S7, S8) (Fig. 11). All the data were standardized by using the Z-score method before the analysis. The results show that PC1 contributes 84.9% of the variance to the analysis of the radius and 86.4% of the variance of to the analysis of the metacarpal. The loading of every measured item is positive in PC1, indicating that

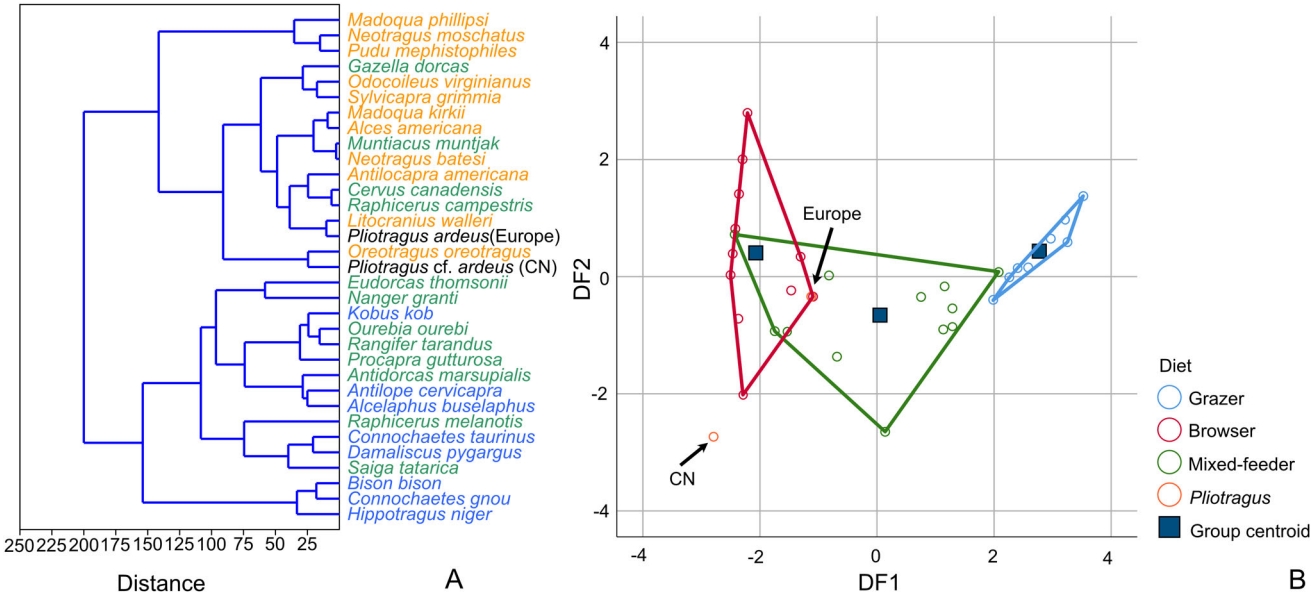

Figure 10. **A,** Cluster analysis and **B,** discriminant function analysis based on the mesowear scores from Carranza-Castañeda and Jiménez-Hidalgo (2021). The colours in A represent browsers (orange), mixed-feeders (green) and grazers (blue). See also Supplemental material Table S6.

the size of these two bones could inform on its habitat. The large heavy bovids inhabiting plains, such as *Megalovis* and early bovines (*Eobison*, *Leptobos*) and the typical mountain climbers (*Gallogoral*, *Procamptoceras*, *Nemorhaerus*, *Capricornis*) can be distinguished from each other by having a positive PC1 and a negative PC1, respectively. The PC2 is the second largest contributor, with 13.1% of the variance of to the analysis of the radius and 10.9% of the variance to the analysis of the metacarpal. Except for the loading of the DAP_dist which is positive, other measured items are negative in PC2 in the analysis of the radius. In the analysis of the metacarpal, PC2 is affected positively by DLM_1_2_diaph and DLM_diaph_min, and negatively by the other variables, indicating that the robustness of the diaphysis has positive influence on PC2. The position of *P. ardeus* in the analysis of the radius and metacarpal is between the group inhabiting plain habitats (*Bison*, *Leptobos*, *Megalovis*) and the group inhabiting mountain habitats (*Gallogoral*, *Procamptoceras*, *Nemorhaerus*, *Capricornis*) on PC1, indicating its medium size. However, the analysis of the radius of *P. ardeus* displays a closer distance to *Bison*, *Leptobos* and *Megalovis* on PC2, indicating that it has a relatively robust distal diaphysis of the radius; the analysis of the metacarpal of *P. ardeus* exhibits a closer distance to

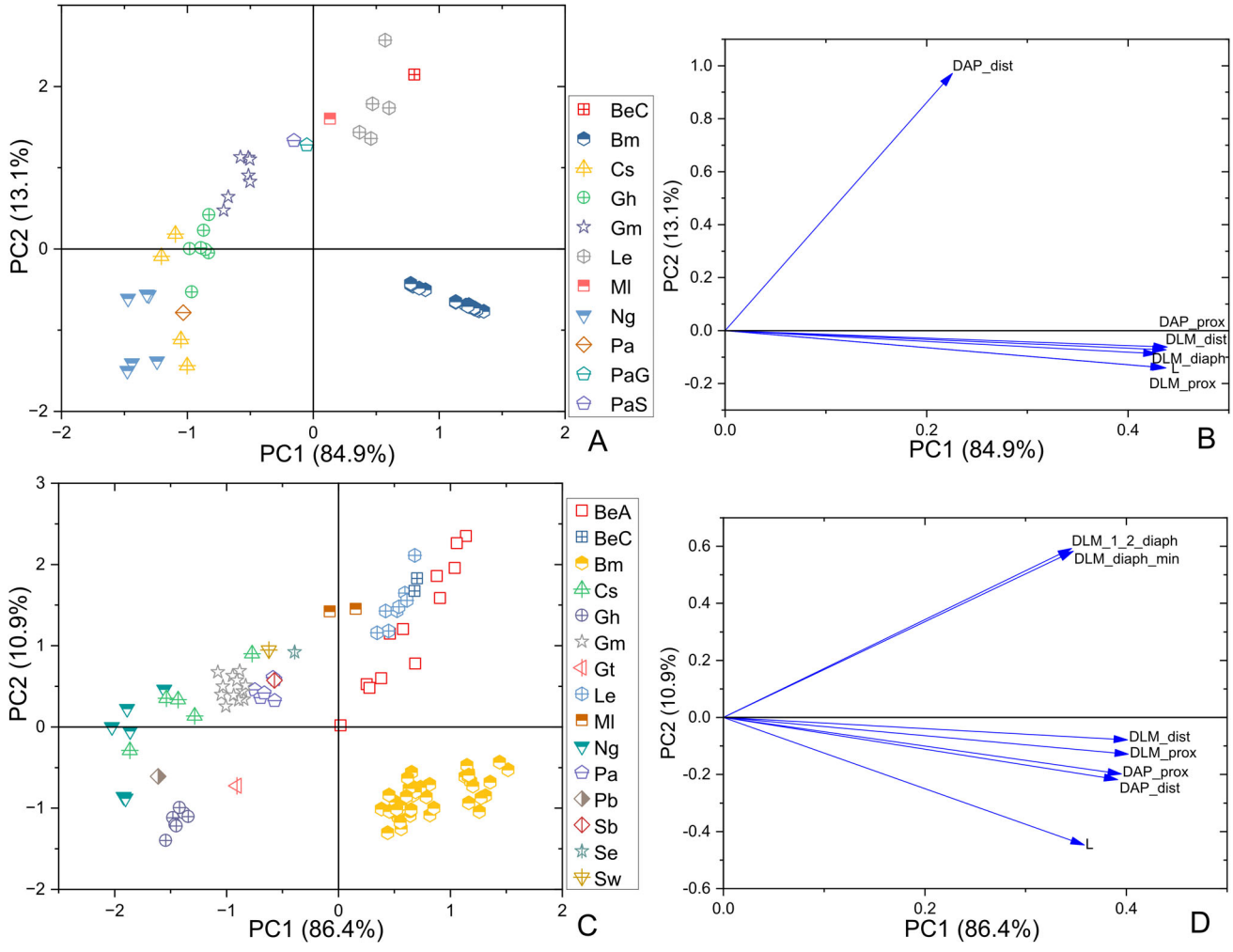

Figure 11. Principal component analysis plots of **A,** metacarpal and **C,** radius bones of *Pliotragus ardeus* and other bovids, illustrating various ecomorphological specializations of the limb bones. A and C are PCA plots with the first two principal components; B and D are the loading plots of each measurement item. **Abbreviations: BeA**, *Bison* (*Eobison*) sp. from Apollonia 1; **BeC**, *Bison* (*Eobison*) sp. from Capena; **Bm**, *Bison menneri*; **Cs**, *Capricornis sumatraensis*; **DAP_dist**, depth of distal epiphysis; **DAP_prox**, depth of proximal epiphysis; **DLM_diaph**, breadth of diaphysis; **DLM_dist**, breadth of distal diaphysis; **DLM_prox**, breadth of proximal epiphysis; **Gm**, *Gallogoral meneghinii*; **Gt**, *Gazellospira torticornis*; **Gth**, *G. torticornis hispanica*; **L**, length; **Le**, *Leptobos etruscus*; **Ng**, *Nemorhedus goral*; **Ml**, *Megalovis latifrons*; **Mp**, *Megalovis pivetaui*; **Pa**, *Pliotragus ardeus*; **PaG**, *Pliotragus ardeus* from Valea Grăunceaului; **PaS**, *P. ardeus* from Senèze; **Pb**, *Procamptoceras brivatense*; **Poa**, *Pontoceros ambiguus*; **Sb**, *Soergelia brigittae*; **Se**, *Soergelia elisabethae*; **Sw**, *Spirocerus wongi*. See also Supplemental material Tables S7, S8.

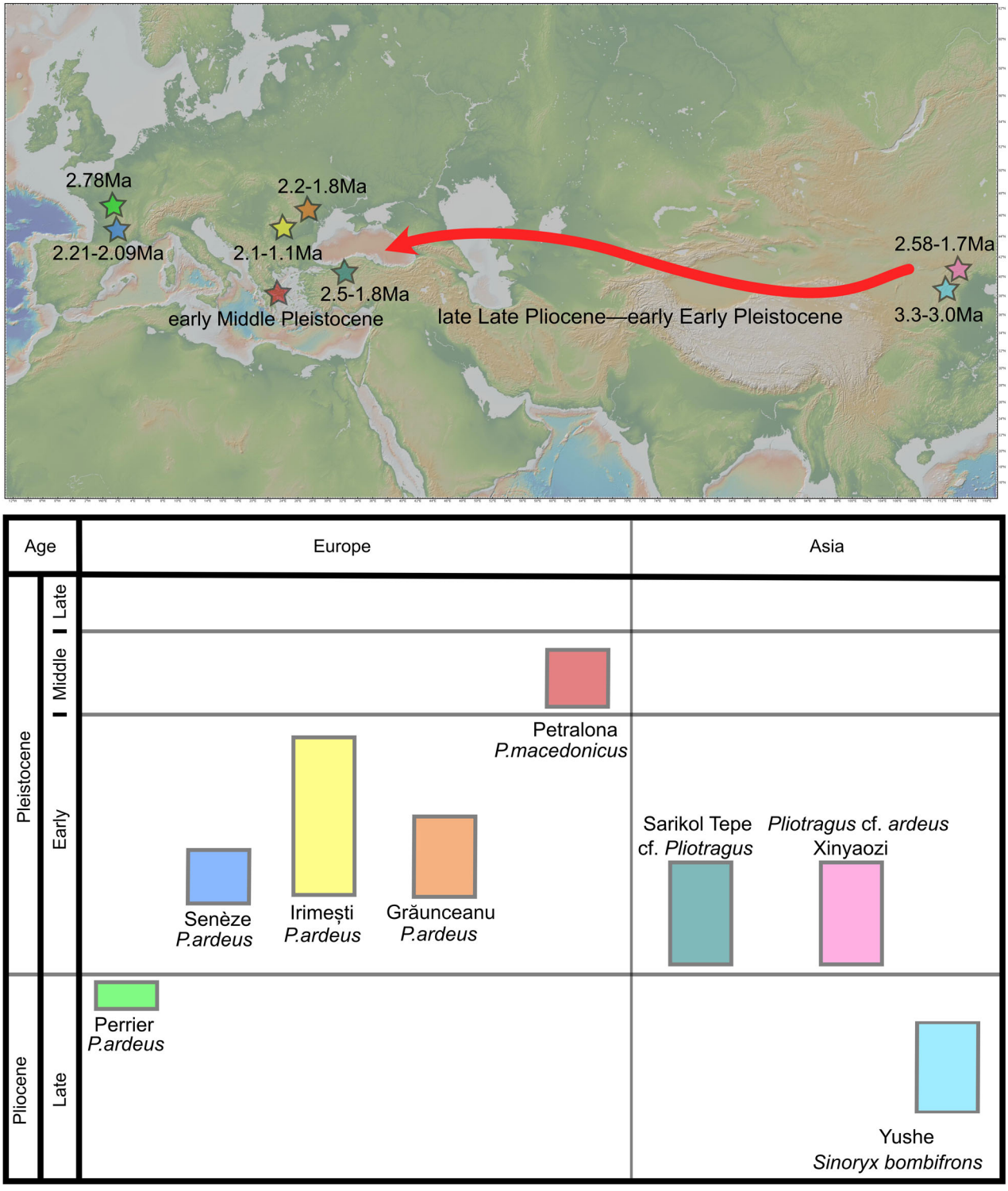

Figure 12. Stratigraphical and geographical distribution of *Pliotragus ardeus* globally. Chronostratigraphical and biochronological correlations based on: Crégut-Bonnoure (2007); Croitor et al. (2024); Gentry (2001); Kostopoulos and Sen (1999); Liu (1989); Nomade et al. (2014); Opdyke et al. (2013). The colours on the biostratigraphical plot correspond to stars on the geographical map. *Sinoryx bombifrons* is shown here because it is a probable synonym of *P. ardeus.*

Gallogoral, *Procamptoceras*, *Nemorhaerus* and *Capricornis* on PC2, indicating its relatively slender metacarpal. According to the PCA, we considered that *P. ardeus* might have inhabited a transitional habitat between plains and mountains or been adapted to both habitats.

Nomade et al. (2014) established the French Plio-Pleistocene biostratigraphical scheme using the $^{40}Ar/^{39}Ar$ method and inferred a palaeoenvironmental transition from 'woodland' to 'open savannah' during that period based on the mammalian fossil record. The presence of *Pliotragus ardeus* in the biostratigraphical sequence from Perrier to Senèze indicates its adaptation to varying palaeoecological conditions, from warm to cold climates, corresponding with the hypothesis proposed by Croitor et al. (2024). The palaeoecology of the Nihewan Basin is similar to that of the French sites from Perrier to Senèze during the Plio-Pleistocene, influenced by general climatic cooling following the onset of Northern Hemisphere glaciations. Around 2.6 Ma, the climate in the Nihewan Basin became cold and dry (Li et al., 2019), leading to the emergence of a mixed savannah and woodland environment (Ao et al., 2013). Considering the palaeohabitat of *P. ardeus* discussed earlier, this species existed in the Early Pleistocene of the Xinyaozi region, typically inhabiting both savannah with scattered forest environments and mountainous areas (Xionger Mountain).

Biostratigraphical and palaeobiogeographical distribution of *Pliotragus*

Hitherto, most specimens of *Pliotragus* have been discovered from Upper Pliocene to Lower Pleistocene deposits in Europe, including *P. ardeus* (Bolomey, 1965; Crégut-Bonnoure, 2025; Croitor et al., 2024; Depéret, 1884; Duvernois & Guérin, 1989; Schaub, 1923) and *P. macedonicus* (Crégut-Bonnoure & Tsoukala, 2005). The definitive earliest record of *Pliotragus* dates to the late Late Pliocene (*c.* 2.78 Ma) from Perrier in France (Depéret, 1884; Nomade et al., 2014). The latest record is represented by *P. macedonicus* from the early Middle Pleistocene of Greece (Crégut-Bonnoure & Tsoukala, 2005); however, the classification of this species as *Pliotragus* requires further discussion. Additionally, Gentry (2001) reported a partial frontal with a pair of horncores found in Austria; however, the stratigraphical horizon of this specimen is unknown, and its assignment to *Pliotragus* requires further evidence. Beyond Europe, the fossil record of *Pliotragus* tentatively includes isolated dental material from the Early Pleistocene (2.5–1.8 Ma) of Turkey, classified as cf. *Pliotragus* based on the similarity of teeth morphology and measurements (Kostopoulos & Sen, 1999). The biostratigraphical position and distribution of *Pliotragus* are shown in Figure 12, arranged geographically from west to east.

The geographical origin and dispersal patterns of *Pliotragus* have been uncertain until now. New findings from China not only expand the known distribution of *Pliotragus* but also highlight the incomplete state of our knowledge regarding the biogeography and distribution of this bovid genus. If we consider *S. bombifrons* as an ancestral form or synonym of *P. ardeus*, the origin of the *Pliotragus* lineage could have also occurred in eastern Asia. The genus dispersed westward from China to Europe during the late Late Pliocene to early Early Pleistocene (Fig. 12). The extinction of *Pliotragus* was most likely associated with the end-Villafranchian event, which was marked by the disappearance of all Pliocene faunal holdovers in the Palearctic Realm (Brugal & Croitor, 2007).

Conclusions

The studied materials from Xinyaozi, including skulls and mandibles, were identified as *Pliotragus* cf. *ardeus*. These specimens are similar to European samples in their cranial morphology and tooth measurements. However, slight differences in the horncores prompted us to classify the Xinyaozi materials as a conformis species of *P. ardeus*.

Based on materials found by previous researchers, we consider *P. ardeus* as a valid species that should be placed into Caprini, having a closer relationship to *Ovibos* than *Rupicapra*. Additionally, the possible synonymy of *Pliotragus ardeus* and *Sinoryx bombifrons* requires further discussion and an analysis based on more evidence is needed. The palaeodiet and palaeohabitat of *Pliotragus* were reconstructed by using measurements of teeth, hypsodonty index of m3, mesowear analysis of teeth and principal component analysis of limb bones. This species is likely a browser-dominated or mixed feeder, adapted to both mountains and plains.

Finally, we summarized the biostratigraphical position and distribution of the genus, suggesting that it might originate in eastern Asia and that it dispersed from China to Europe during the late Late Pliocene to early Early Pleistocene.

Acknowledgements

The authors are grateful to Prof. Qi Wei for providing the specimens from Xinyaozi for this study. We also

thank Profs Zhaoqun Zhang and Haowen Tong from IVPP for their fruitful discussions, and Prof. Shiqi Wang from IVPP who provided the 3D model of the cast of *Sinoryx bomifrons* for comparison. We appreciate very much Dr Evelyne Crégut-Bonnoure from Muséum Requien for sharing with us her unpublished data with the most important material of *Pliotragus ardeus* in Europe. Finally, the authors are deeply thankful to Drs Dimitris S. Kostopoulos and Faysal Bibi for their significant comments and suggestions to improve the manuscript. This work was supported by the National Natural Science Foundation of China (No. 42402001), National Key Research and Development Program of China (No. 2023YFF0804501) and the Science Foundation of Hebei Normal University (No. L2023B54).

Disclosure statement

No potential conflict of interest was reported by the author(s).

Supplemental material

Supplemental material for this article can be accessed online here: https://doi.org/10.1080/14772019.2025.2518101.

Data availability statement

The data that support the findings of this study are openly available in MorphoBank at https://doi.org/10.7934/P5892 (Bai et al., 2025).

References

Ao, H., **An, Z.**, **Dekkers, M. J.**, **Li, Y.**, **Xiao, G.**, **Zhao, H.**, & **Qiang, X.** (2013). Pleistocene magnetochronology of the fauna and Paleolithic sites in the Nihewan Basin: Significance for environmental and hominin evolution in North China. *Quaternary Geochronology*, *18*, 78–92. https://doi.org/10.1016/j.quageo.2013.06.004

Bai, W., **Croitor, R.**, **Zhang, L.** & **Dong, W.** (2025). Data from: The first record of *Pliotragus* (Artiodactyla: Bovidae) in the Early Pleistocene of eastern Asia; contribution to its systematics, palaeohabitat, and palaeobiogeography. Morphobank. https://doi.org/10.7934/P5892

Bai, W., **Dong, W.**, **Liu, W.**, **Zhang, L.**, **Li, L.**, & **Li, Q.** (2022). Pleistocene hedgehog *Mesechinus* (Eulipotyphla, Mammalia) in China. *Journal of Mammalian Evolution*, *29*, 797–814. https://doi.org/10.1007/s10914-022-09612-w

Bai, W., **Dong, W.**, & **Zhang, L.** (2024). The first confirmation of North American extinct shrub-ox (*Euceratherium*, Artiodactyla, Mammalia) in the Early Pleistocene of northern China. *Quaternary Science Reviews*, *336*, 108777. https://doi.org/10.1016/j.quascirev.2024.108777

Bai, W., **Dong, W.**, **Zhang, L.**, **Wei, Q.**, **Liu, W.**, & **Chen, Z.** (2019). New material of the Early Pleistocene spiral horned antelope *Spirocerus* (Artiodactyla, Mammalia) from North China and discussion on its evolution. *Quaternary International*, *522*, 94–102. https://doi.org/10.1016/j.quaint.2019.06.029

Bai, W., **Wang, X.**, & **Dong, W.** (2024). Gazelles (Mammalia: Bovidae) from the early Pleistocene Tianzhen area, Shanxi Province, China. *Historical Biology*, *36*, 1639–1654. https://doi.org/10.1080/08912963.2023.2222131

Bärmann, E. V. (2012). *Toward a comprehensive phylogeny of Bovidae (Ruminantia, Artiodactyla, Mammalia)* University of Cambridge]. Cambridge.

Bärmann, E. V., & **Rössner, G. E.** (2011). Dental nomenclature in Ruminantia: Towards a standard terminological framework. *Mammalian Biology*, *76*, 762–768. https://doi.org/10.1016/j.mambio.2011.07.002

Bohlin, B. (1935). Cavicornier der Hipparion-Fauna Nord-Chinas. *Palaontologia Sinica*, *Series C*, *9*, 1–166.

Bohlin, B. (1938). Einige jungtertiäre und Pleistozäne cavicornier aus nord-China. *Nova Acta Regiae Societatis Scientiarum Upsaliensis*, *11*, 1–50.

Bolomey, A. (1965). Contribution à la connaissance de la morphologie de *Pliotragus ardeus*. *Revue Roumaine de Biologie*, *Série de Zoologie*, *10*, 319–323.

Brugal, J. P., & **Croitor, R.** (2007). Evolution, ecology and biochronology of herbivore associations in Europe during the last 3 million years. *Quaternaire*, *18*, 129–152. https://doi.org/10.4000/quaternaire.1014

Carranza-Castañeda, O., & **Jiménez-Hidalgo, E.** (2021). Pliocene Antilocapridae (Mammalia: Artiodactyla) from San Miguel de Allende, Guanajuato, central Mexico. *Journal of South American Earth Sciences*, *112*, 103571. https://doi.org/10.1016/j.jsames.2021.103571

Chen, G., & **Zhang, Z.** (2007). Restudy of Chinese fossil bovids referred to *Protoryx* (Bovidae, Artiodactyla). *Vertebrata PalAsiatica*, *45*, 98–109.

Crégut-Bonnoure, E. (2007). Apport des Caprinae et Antilopinae (Mammalia, Bovidae) à la biostratigraphie du Pliocène terminal et du Pléistocène d'europe. *Quaternaire*, *18*, 73–97. https://doi.org/10.4000/quaternaire.996

Crégut-Bonnoure, E. (2025). The Bovidae (Mammalia, Artiodactyla) from Senèze. In E. Delson, M. Faure, C. Guérin (Eds.), *Senèze: Life in Central France Around Two Million Years Ago* (pp. 433–585). Springer.

Crégut-Bonnoure, E., & **Dimitrijevic, V.** (2006). *Megalovis balcanicus* sp. nov. and *Soergelia intermedia* sp. nov. (Mammalia, Bovidae, Caprinae), new Ovibovini from the Early Pleistocene of Europe. *Revue de Paléobiologie*, *25*, 723–773.

Crégut-Bonnoure, E., & **Tsoukala, E.** (2005). The Pleistocene bovids from Petralona Cave (Macedonia, Greece): new interpretations and biogeographical implications. *Quaternaire*, *2* (suppl.), 161–178.

Croitor, R., **Robinson, C.**, **Curran, S.**, **Terhune, C.**, **Drăguşin, V.**, **Pobiner, B.**, **Popescu, A.**, & **Petculescu, A.** (2024). Early Pleistocene ruminants (Artiodactyla, Mammalia) from the Dacian Basin (South Romania)

before and after the Pachycrocuta event: implications for hominin dispersals in Western Eurasia. *Historical Biology*, *36*, 485–533. https://doi.org/10.1080/08912963.2023.2167602

Deng, T., & **Xue, X.** (1999). *Chinese fossil horse of Equus and their environment*. China Ocean Press.

Depéret, C. (1884). Nouvelles Études sur les Ruminants pliocènes et quaternaires d'Auvergne. *Bulletin de la Société géologique de France*, *12*, 247–284.

Dong, W., **Bai, W.**, **Liu, W.**, & **Zhang, L.** (2023). The first description of Equidae (Perissodactyla, Mammalia) from Xinyaozi Ravine in Shanxi, North China. *Vertebrata PalAsiatica*, *61*, 212–244.

Dong, W., **Bai, W.**, **Pan, Y.**, & **Liu, W.** (2020). New material of Cervidae (Artiodactyla, Mammalia) from Xinyaozi Ravine in Shanxi, North China. *Vertebrata PalAsiatica*, *58*, 221–248.

Dong, W., **Bai, W.**, & **Zhang, L.** (2021). The first description of Rhinocerotidae (Perissodactyla, Mammalia) from Xinyaozi Ravine in Shanxi, North China. *Vertebrata PalAsiatica*, *59*, 273–294.

Dong, W., **Wei, Q.**, **Bai, W.**, **Zhang, L.**, **Liu, W.**, **Chen, Z.**, **Bai, Y.**, & **Wu, Y.** (2019). New material of the Early Pleistocene *Elaphurus* (Artiodactyla, Mammalia) from North China and discussion on taxonomy of *Elaphurus*. *Quaternary International*, *519*, 113–121. https://doi.org/10.1016/j.quaint.2018.05.015

Duvernois, M. P., & **Guérin, C.** (1989). Les Bovidae (Mammalia, Artiodactyla) du Villafranchien supérieur d'europe occidentale. *Geobios*, *22*, 339–379. https://doi.org/10.1016/S0016-6995(89)80136-6

Fang, Y., **Dong, W.**, & **Tang, G.** (2004). Early Pleistocene Bovidae (Artiodactyla, Mammalia) from the Tuozidong at Tangshan, Jiangsu Province, China. In W. Dong (Ed.), *Proceedings of the Ninth Annual Symposium of the Chinese Society of Vertebrate Paleontology* (pp. 69–81). China Ocean Press.

Fortelius, M., & **Solounias, N.** (2000). Functional characterization of ungulate molars using the abrasion-attrition wear gradient: a new method for reconstructing paleodiets. *American Museum Novitates*, 2000, 1–36. https://doi.org/10.1206/0003-0082(2000)301<0001:FCOUMU>2.0.CO;2

Fraser, D., **Zybutz, T.**, **Lightner, E.**, & **Theodor, J.** (2014). Ruminant mandibular tooth mesowear: a new scheme for increasing paleoecological sample sizes. *Journal of Zoology*, *294*, 41–48. https://doi.org/10.1111/jzo.12149

Gentry, A. W. (1970). Revised classification for *Makapania broomi* Wells and Cooke (Bovidae, Mammalia). *Palaeontologia africana*, *13*, 63–67.

Gentry, A. W. (1971). The earliest goats and other antelopes from Samos *Hipparion* Fauna. *Bulletin of the British Museum (Natural History)*, *Geology*, *20*, 229–296.

Gentry, A. W. (2001). An Ovibovine (Mammalia, Bovidae) from the Neogene of Stratzing, Austria. *Annalen des Naturhistorischen Museums in Wien*, *102A*, 189–199.

Gray, J. E. (1821). On the natural arrangement of vertebrose animals. *London Medical Repository*, *15*, 296–310.

Groves, C., & **Grubb, P.** (2011). *Ungulate taxonomy*. The Johns Hopkins University Press.

Guérin, C. (1965). *Gallogoral* (nov. gen.) *meneghinii* (Rütimeyer, 1878). Un Rupicapriné du Villafranchien d'Europe occidentale. *Documents des Laboratoires de Géologie de la Faculté des Sciences de Lyon*, *11*, 1–353.

Hammer, Ø., **Harper, D. A. T.**, & **Ryan, P. D.** (2001). PAST: paleontological statistics software package for education and data analysis. *Palaeontologia Electronica*, *4*, 1–9.

Hassanin, A., **Delsuc, F.**, **Ropiquet, A.**, **Hammer, C.**, **van Vuuren, B. J.**, **Matthee, C.**, **Ruiz-Garcia, M.**, **François, C.**, **Areskoug, V.**, **Nguyen, T. T.**, & **Couloux, A.** (2012). Pattern and timing of diversification of Cetartiodactyla (Mammalia, Laurasiatheria), as revealed by a comprehensive analysis of mitochondrial genomes. *Comptes Rendus Biologies*, *335*, 32–50. https://doi.org/10.1016/j.crvi.2011.11.002

Kostopoulos, D. S. (1997). The Plio-Pleistocene artiodactyls of Macedonia 1. The fossiliferous site Apollonia-1, Mygdonia basin of Greece. *Geodiversitas*, *19*, 845–875.

Kostopoulos, D. S. (2009). The Late Miocene mammal faunas of the Mytilinii Basin, Samos Island, Greece: New Collection 14. Bovidae. *Beiträge zur Paläontologie*, *31*, 345–389.

Kostopoulos, D. S. (2022). The fossil record of Bovids (Mammalia: Artiodactyla: Ruminantia: Pecora: Bovidae) in Greece. In E. Vlachos (Ed.), *Fossil Vertebrates of Greece. Vol. 2* (pp. 113–203). Springer.

Kostopoulos, D. S., & **Sen, S.** (1999). Late Pliocene (Villafranchian) mammals from Sarikol Tepe, Ankara, Turkey. *Mitteilungen der Bayerischen Staatssammlung für Paläontologie und Histor. Geologie*, *39*, 165–202.

Kretzoi, M, (1941). Ősemlősmaradványok Betfiáról. *Földtani Közlöny*, *71*, 235–261.

Lewis, P. O. (2001). A likelihood approach to estimating phylogeny from discrete morphological character data. *Systematic Biology*, **50**, 913–925. https://doi.org/10.1080/106351501753462876

Li, Y., **Zhang, Z.**, **Ding, G.**, **Xu, Q.**, **Wang, Y.**, **Chi, Z.**, **Dong, J.**, & **Zhang, L.** (2019). Late Pliocene and early Pleistocene vegetation and climate change revealed by a pollen record from Nihewan Basin, North China. *Quaternary Science Reviews*, *222*, 105905. https://doi.org/10.1016/j.quascirev.2019.105905

Liu, X. (1989). Lower Pleistocene and its lower boundary in 'Nihewan Formation'. In Z. G. Yang & H. M. Lin (Eds.), *Quaternary Processes and Events in China Offshore and Onshore Areas* (pp. 143–154). China Ocean Press.

Matsumoto, H. (1926). On a new fossil race of bighorn sheep from Shantung, China. *The Science reports of the Tohoku Imperial University*, *10*, 38–41.

Mendoza, M., **Janis, C. M.**, & **Palmqvist, P.** (2002). Characterizing complex craniodental patterns related to feeding behaviour in ungulates: a multivariate approach. *Journal of Zoology*, *258*, 223–246. https://doi.org/10.1017/S0952836902001346

Nomade, S., **Pastre, J.**, **Guillou, H.**, **Faure, M.**, **Guérin, C.**, **Delson, E.**, **Debard, E.**, **Voinchet, P.**, & **Messager, E.** (2014). $^{40}Ar/^{39}Ar$ constraints on some French landmark Late Pliocene to Early Pleistocene large mammalian paleofaunas: Paleoenvironmental and paleoecological implications. *Quaternary Geochronology*, *21*, 2–15. https://doi.org/10.1016/j.quageo.2012.12.006

Ogino, S., **Takai, M.**, **Nakaya, H.**, & **Hongo, H.** (2009). Artiodactyl specimens from the Udunga fauna. *Asian Paleoprimatology*, *5*, 105–129.

Opdyke, N., **Huang, K.**, **Tedford, R. H.** (2013). Erratum To: The Paleomagnetism and Magnetic Stratigraphy of the Late Cenozoic Sediments of the Yushe Basin, Shanxi

Province, China. In: R. H. Tedford., Z. X. Qiu & L. J. Flynn (Eds.), *Late Cenozoic Yushe Basin, Shanxi Province, China: Geology and Fossil Mammals Volume I: History, Geology, and Magnetostratigraphy* (pp. E1–E3). Springer.

Owen, R. (1848). Description of teeth and portions of jaw of two extinct anthracotherioid quadrupeds (*Hyopotamus vectianus* and *Hyop. bovines*) discovered by the Marchioness of Hastings in the Eocene deposits on the NW coast of the Isle of Wight: with an attempt to develop Cuvier's idea of the classification of pachyderms by the number of their toes. *Quarterly Journal of the Geological Society of London*, *4*, 103–141. https://doi.org/10.1144/GSL.JGS.1848.004.01-02.21

Qiu, Z. (2002). *Hesperotherium* – A new genus of the last chalicotheres. *Vertebrata PalAsiatica*, *40*, 317–325.

Qiu, Z., **Wei, Q.**, **Pei, S.**, & **Chen, Z.** (2002). Preliminary report on *Postschizotherium* (Mammalia: Hyarcoidea) material from Tianzhen, Shanxi, China. *Vertebrata PalAsiatica*, *4*, 146–160.

Rodrigo, M. A. (2011). Los bóvidos Villafranquienses de La Puebla de Valverde y Villarroya: sistemática, filogenia y paleobiología Universidad de Zaragoza]. Zaragoza.

Ronquist, F., **Klopfstein, S.**, **Vilhelmsen, L.**, **Schulmeister, S.**, **Murray, D. L.**, **Rasnitsyn, A. P.** (2012). A total-evidence approach to dating with fossils, applied to the early radiation of the *Hymenoptera*. *Systematic Biology*, *61*, 973–999. https://doi.org/10.1093/sysbio/sys058

Ronquist, F., **Teslenko, M.**, **van der Mark, P.**, **Ayres, D. L.**, **Darling, A.**, **Höhna, S.**, **Larget, B.**, **Liu, L.**, **Suchard, M. A.**, & **Huelsenbeck, J. P.** (2012). MrBayes 3.2: efficient Bayesian phylogenetic inference and model choice across a large model space. *Systematic Biology*, *61*, 539–542. https://doi.org/10.1093/sysbio/sys029

Schaub, S. (1923). Neue und wenig bekannte Cavicornier von Senèze. *Eclogae Geologicae Helvetiae*, *18*, 281–290.

Schaub, S. (1943). Die oberpliocaene Säugetierfauna von Senèze (Haute-Loire) und ihre verbreitungsgeschichtliche Stellung. *Eclogae Geologicae Helvetiae*, *36*, 270–289.

Sher, A. V. (1997). An early quaternary *Bison* population from Untermassfeld: *Bison menneri* sp. nov. In R. D. Kahlke, (Ed.), *Das Pleistozän Von Untermassfeld bei Meningen (Thüringen)* (pp. 101–180). Propylaeum.

Simpson, G. G. (1945). The principles of classification and a classification of mammals. *Bulletin of the American Museum of Nature History*, *85*, 1–350.

Sokolov, I. I. (1953). Essay for a natural classification of the Cavicornians (Bovidae). *Transactions of Zoological Institute*, *14*, 1–295.

Teilhard de Chardin, P., & **Piveteau, J.** (1930). Les mammifères fossiles de Nihowan (Chine). *Annales de Paléontologie*, *19*, 1–134.

Teilhard de Chardin, P., & **Trassaert, M.** (1938). Cavicornia of south-eastern Shansi. *Paleontologia Sinica*, *New Series C*, *6*, 1–110.

Tong, H., **Zhang, B.**, **Chen, X.**, & **Wang, X.** (2022). New fossils of small and medium-sized bovids from the Early Pleistocene site of Shanshenmiaozui in Nihewan Basin, North China. *Vertebrata PalAsiatica*, *60*, 134–168.

Viret, J. (1961). Artiodactyla. In J. Piveteau (Ed.), *Traité de Paléontologie VI*, *Vol. 1* (pp. 1038–1084). Masson et Cie.

Vislobokova, I., **Dmitrieva, E.**, & **Kalmykov, N.** (1995). Artiodactyls from the late Pliocene of Udunga, western trans-baikal, Russia. *Journal of Vertebrate Paleontology*, *15*, 146–159. https://doi.org/10.1080/02724634.1995.10011214

Wang, S., **Sun, J.**, **Li, C.**, **Li, S.**, **Fu, J.**, **Jiangzuo, Q.**, **Xing, L.**, & **Yang, R.** (2023). Discovery of a fossil dwarf antelope outside of Africa and its implications for the late Miocene ecosystem in the northeast margin of the Tibetan Plateau. *Gondwana Research*, *113*, 102–115. https://doi.org/10.1016/j.gr.2022.10.012

Xie, J., **Chen, Y.**, **Cai, G.**, **Cai, R.**, **Hu, Z.**, & **Wang, H.** (2023). Tree Visualization By One Table (tvBOT): a web application for visualizing, modifying and annotating phylogenetic trees. *Nucleic Acids Research*, *51*, W587–W592. https://doi.org/10.1093/nar/gkad359

Zhang, C., **Stadler, T.**, **Klopfstein, S.**, **Heath, T. A.**, **Ronquist, F.** (2016). Total-evidence dating under the fossilized birth–death process. *Systematic Biology*, **65**, 228–249. https://doi.org/10.1093/sysbio/syv080

Associate Editor: Guillaume Billet